

NASA CR-1181

ANALYSIS OF GEOMETRY AND DESIGN POINT PERFORMANCE OF  
AXIAL FLOW TURBINES

I - Development of the Analysis Method and the  
Loss Coefficient Correlation

By A. F. Carter, M. Platt, and F. K. Lenherr

Distribution of this report is provided in the interest of  
information exchange. Responsibility for the contents  
resides in the author or organization that prepared it.

Prepared under Contract No. NAS 3-9418 by  
NORTHERN RESEARCH AND ENGINEERING CORPORATION  
Cambridge, Mass.

for Lewis Research Center

NATIONAL AERONAUTICS AND SPACE ADMINISTRATION

---

For sale by the Clearinghouse for Federal Scientific and Technical Information  
Springfield, Virginia 22151 - CFSTI price \$3.00



PRECEDING PAGE BLANK NOT FILMED.

## FOREWORD

The research described herein, which was conducted by Northern Research and Engineering, was performed under NASA Contract NAS 3-9418. The work was done under the technical management of Mr. Edward L. Warren, Air-breathing Engines Division, NASA-Lewis Research Center, with Mr. Arthur J. Glassman, Fluid System Components Division, NASA-Lewis Research Center, as technical consultant. Dr. D. M. Dix directed the work for Northern Research and Engineering. The report was originally issued as Northern Research and Engineering Report 1125-1, September 1967.



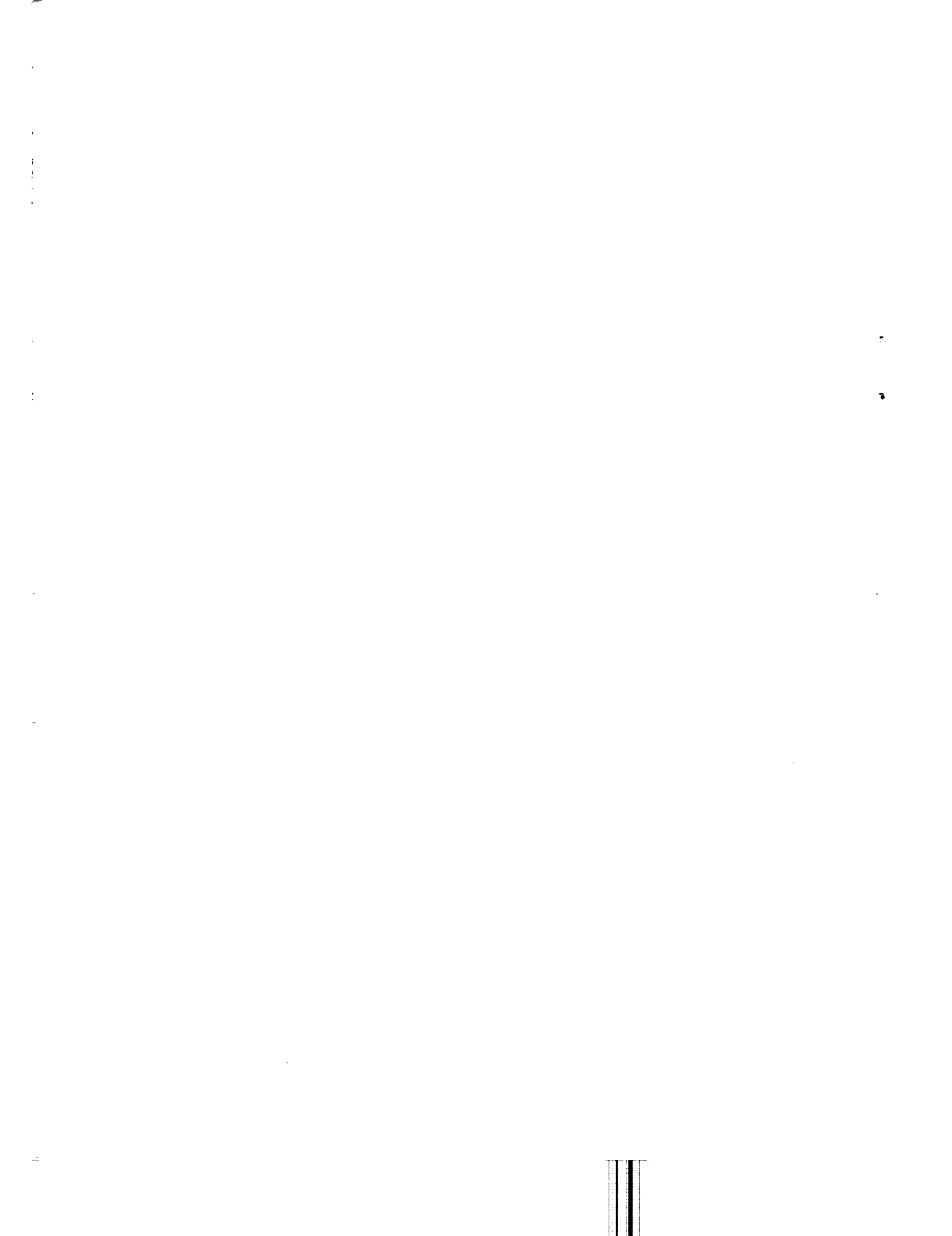
TABLE OF CONTENTS

SUMMARY . . . . .	1
INTRODUCTION . . . . .	2
Report Arrangement . . . . .	5
THE STREAM-FILAMENT APPROACH TO TURBINE DESIGN . . . . .	6
Introduction . . . . .	6
Analysis Along Streamlines . . . . .	7
The Continuity Equation . . . . .	14
The Radial Equilibrium Equation . . . . .	16
MODIFICATIONS TO THE STREAM-FILAMENT APPROACH FOR VARYING SPECIFIC HEAT, MIXING, AND COOLANT FLOWS . . . . .	21
Introduction . . . . .	21
Variations of Specific Heat . . . . .	22
Mixing . . . . .	24
Coolant Flows . . . . .	28
Concluding Remarks . . . . .	31
DEVELOPMENT OF THE LOSS CORRELATION . . . . .	34
Introduction . . . . .	34
Data for the Loss Correlation . . . . .	35
Correlation of Total-Pressure-Loss Coefficient . . . . .	40
Mean-Line Stage Performance Prediction Utilizing Loss Coefficient Correlation . . . . .	44
Stream-Filament Prediction of Stage Performance . . . . .	46
Loss Factors . . . . .	48
Kinetic-Energy-Loss Coefficients . . . . .	50

DEVELOPMENT OF THE ANALYSIS PROCEDURE . . . . .	52
Introduction . . . . .	52
Specification of the Design Requirements and Analysis Variables . . . . .	53
Basic Equations and Fundamental Solution Technique . . . . .	57
Over-All Solution Procedure . . . . .	66
Results of the Analysis . . . . .	68
REFERENCES . . . . .	72
NOMENCLATURE . . . . .	73
APPENDICES	
I: THE RELATIONSHIP BETWEEN TOTAL-PRESSURE-LOSS COEFFICIENT AND KINETIC-ENERGY-LOSS COEFFICIENT . . . . .	76
II: COEFFICIENTS FOR THE EVALUATION OF MERIDIONAL VELOCITY DISTRIBUTION AT ANY DESIGN PLANE . . . . .	81
III: THE COEFFICIENTS OF THE TOTAL-PRESSURE-LOSS COEFFICIENT DERIVATIVE . . . . .	88

## LIST OF FIGURES

Figure 1:	Meridional Section of a Two-Stage Turbine to Diagrammatically Illustrate Axisymmetric Streamline Flow . . . . .	74
Figure 2:	Nomenclature for Axisymmetric Flow in an Arbitrary Turbine Annulus . . . . .	75
Figure 3:	Turbine Velocity Triangle Nomenclature Used in the Stream-Filament Analysis . . . . .	76
Figure 4:	A Simple Correlation of Achievable Turbine Efficiency (Zero Tip Leakage) . . . . .	77
Figure 5:	Loss Coefficients Versus Row Deflection . . . . .	78
Figure 6:	Loss Coefficients Versus Row Reaction . . . . .	79
Figure 7:	Loss Coefficients Versus Row Exit Angle . . . . .	80
Figure 8:	Reduced Loss Coefficients Versus Velocity Ratio . . . . .	81
Figure 9:	Reduced Loss Coefficients with Additional Exit Angle Correction Versus Velocity Ratio . . . . .	82
Figure 10:	A Comparison of Test Data Efficiencies with Prediction Values Using Alternative Loss Coefficient Correlations ( $g_0 \sqrt{c_p \Delta T_0} / u^2 = 1.0$ ) . . . . .	83
Figure 11:	A Comparison of Test Data Efficiencies with Prediction Values Using Alternative Loss Coefficient Correlations ( $g_0 \sqrt{c_p \Delta T_0} / u^2 = 1.5$ ) . . . . .	84
Figure 12:	A Comparison of Test Data Efficiencies with Prediction Values Using Alternative Loss Coefficient Correlations ( $g_0 \sqrt{c_p \Delta T_0} / u^2 = 2.0$ ) . . . . .	85
Figure 13:	A Comparison of Test Data Efficiencies with Prediction Values Using Alternative Loss Coefficient Correlations ( $g_0 \sqrt{c_p \Delta T_0} / u^2 = 2.5$ ) . . . . .	86
Figure 14:	Predicted Efficiency Contours Based on Row Loss Coefficient Correlation A . . . . .	87
Figure 15:	Predicted Efficiency Contours Based on Row Loss Coefficient Correlation B . . . . .	88





ANALYSIS OF GEOMETRY AND DESIGN POINT  
PERFORMANCE OF AXIAL FLOW TURBINES

PART I - DEVELOPMENT OF THE ANALYSIS METHOD  
AND THE LOSS COEFFICIENT CORRELATION

by A. F. Carter, M. Platt, and F. K. Lenherr

Northern Research and Engineering Corporation

SUMMARY

This report presents the development of a stream-filament analysis procedure and a correlation of total-pressure-loss coefficients which forms the basis for a computer program with which the geometry and design-point performance of axial turbines may be investigated. This report is the first part of a two-part report; the second part will present a complete description of the actual computer program.

Since one of the principal features of the analysis procedure is the solution of the radial equilibrium equation taking into account radial gradients of enthalpy and entropy, the computer program based on this analysis will provide the turbine designer with the freedom to consider arbitrarily selected distributions of tangential velocities (or stator exit angles) and radial distributions of work output as analysis variables. In addition, with the incorporation of a total-pressure-loss coefficient correlation, the computer program which results from the analysis can be used for a systematic investigation of the performance of alternative turbine designs for specified design requirements.

## INTRODUCTION

Until relatively recently, the majority of axial turbines has been designed using an extremely simple approach in which the flow at each of the design stations is assumed to have radially constant values of total temperature and total pressure. With this assumption and the additional assumption that radial components of velocity are zero, the radial equilibrium equation is considerably simplified. One solution of the simple radial equilibrium equation is the irrotational or free-vortex solution in which the axial component of velocity is constant, and the tangential component varies inversely with radius. The principal merits of the free-vortex design of turbines are that the design velocity triangles are readily obtained, and that acceptable levels of performance have been achieved when such designs are suitably bladed.

The principal disadvantages of the free-vortex approach to turbine design are that the model is basically inaccurate and that the design method is very restrictive. Turbine test results from stages designed using the free-vortex method clearly show significant variations in axial velocity, total pressure, and total temperature. It is unrealistic to assume that there will not be significant radial variations of total pressure and temperature when there are large variations in the aerodynamic design parameters and the blade sections from hub to casing in typical turbine designs. The radial variation of the stage aerodynamics of free-vortex turbines is an illustration of the restrictive nature of the simple design approach. With a selected mean-line design of a given reaction and rotor deflection, the reaction and deflection of the remaining sections of the rotor blading are merely functions of the design radius

of these sections and, since no radial variation in temperature drop can be considered, the nondimensional loading factor,  $g_c \mathcal{J} c_p \Delta T_c / U^2$ , rapidly increases towards the hub section of the blade. Thus, the over-all geometry of a turbine is frequently dictated by considerations of the hub loading.

Any free-vortex turbine can be considered as a series of simply related elements, and obviously the freedom of the turbine designer would be considerably increased if the dependence of the over-all design geometry on a selected mean line could be reduced. Consideration of a number of elements over the radial extent of a design forms the basis for a stream-filament analysis of turbine designs; with this approach it is not necessary to select radially constant work extraction or restrict the variation of tangential velocities to a particular type. Unfortunately, a turbine design cannot be considered as a series of independent filaments defined by surfaces generated by the rotation of streamlines about the center line of the machine. The radial locations of the streamlines which define the individual filaments of the flow are dependent on radial equilibrium and mass flow continuity requirements at each of the design stations through the machine. Thus, an essential ingredient of the stream-filament analysis of a turbine design is the simultaneous solution of the radial equilibrium and continuity equations at each of the design stations through a turbine. However, once the decision is made to consider radial variations of enthalpy and entropy and to include the effects of meridional components of streamline slope and curvature, no simple analytical solution of the radial equilibrium equation is possible. Hence, it becomes desirable to use a computer for the solution of the problem and it is, of

course, one of the primary purposes of the present report to develop the analysis such that it forms the basis for a computer program.

Even though the preparation of numerical procedures for the stream-filament analysis of a turbine design is of importance in itself, unless the procedure incorporates soundly based assumptions concerning the losses associated with the elements of the blading, the detailed calculation of interblade row aerodynamics will be of little value. Hence, an essential part of the development of what is fundamentally a design analysis computing system is the development of a loss correlation which will be an integral part of the final computer program. Such a correlation has been developed as part of the over-all analysis. Since the basic requirement is for the analysis of turbine design-point geometry, the correlation obtained is based on the interblade row flow angles and velocities and makes no reference to the detailed design of the blading. The detailed design of the blading will, of course, influence the over-all performance of a turbine, and the correlation of loss coefficient must be regarded as a datum level of loss which a turbine designer may factor as his experience and knowledge of the probable blading dictates.

While the model of streamline flow through a turbine represents a considerable advance from that used in the recent past, it is still a considerable simplification of the extremely complex flow which will occur in an actual turbine. For example, it assumes the flow is axisymmetric and ignores the secondary flow effects. Both are factors which make it unrealistic to assume that the flow which passes between selected adjacent streamlines at the turbine inlet will be identically that which passes between these streamlines at some later design plane. While not attempting

to quantitatively assess the amount of mixing which occurs throughout a turbine, the analysis includes a method by which the effect of mixing can be simulated. An additional factor which is considered in the analysis is the addition of coolant flows to the main stream. Here again, the model which is proposed is a relatively simple one which attempts only a first order correction to the over-all stream-filament approach to account for the addition of mass flow at a temperature level which may differ from that which exists in the main stream at the point of admission. No attempt is made to differentiate between cooling flow which results from disk cooling or blade cooling, be it transpiration or convective cooling.

#### Report Arrangement

The first section of the report outlines the stream-filament approach to turbine design and introduces the basic equations used in the analysis. Modifications to the simple stream-filament approach are then considered. These modifications are undertaken to include in the analysis the effects of changes in specific heat through a turbine as the temperature level falls, the interfilament mixing which occurs within a turbine, and the addition of coolant flows in a high temperature application. The following section discusses the investigation which leads to the selected correlation of total-pressure-loss coefficient which is to be an integral part of the analysis program. In the final section, the analysis is developed to the point where it forms the basis of the computer program.

The relationship between kinetic-energy-loss and total-pressure-loss coefficients and the coefficients of the differential equations to be solved are presented in the appendices.

## THE STREAM-FILAMENT APPROACH TO TURBINE DESIGN

### Introduction

The basic model used for the stream-filament analysis of a turbine design consists of a series of streamlines which trace the path of the flow from known conditions at the inlet to the first stage of the turbine to the final design station at exit from the last blade row. Making the assumption that the flow is axisymmetric throughout the entire turbine, a series of streamlines can be selected at the machine inlet to define a series of annular streamtubes. With the position of the streamlines defined so that adjacent streamline surfaces contain a known fraction of the total flow, the entire flow field throughout the turbine can then be considered as a number of annular elements. Since the flow is assumed axisymmetric, the flow through the turbine can be represented by a meridional section as diagrammatically illustrated in Figure 1.

In general, even for the simplified case in which axial symmetry is assumed, the flow path through the stages of a turbine will be quite complex and will be influenced by a number of factors not the least of which will be the detailed design of the blading. However, for an analysis of the geometry and the design-point performance of possible turbine configurations, the principal objective is to define the blading requirement, and hence the analysis is restricted to design stations immediately upstream and downstream of the blade rows.

With the turbine subdivided into a number of elements, the design of the over-all turbine can be considered as that of a number of individual turbines. Hence, by applying the fundamental turbine design equations to individual sections of the turbine, the stream-filament

approach will permit the specification of the design requirements to element of sections of the turbine analysis. These individual elements, however, cannot be considered in isolation for these are interrelated by considerations of radial equilibrium and the over-all design requirements which include satisfying mass flow continuity at each design station and the specified total power output of each stage. Hence, the principal requirement of a stream-filament analysis of a turbine design is for the solution of the radial equilibrium equation; the solution of the design equations in the streamline direction is a relatively simple task, which is merely an extension of standard turbine design practice to individual streamlines. Since the blade row elemental performance is likely to be a function of radius, and the work output may be specified to vary with radius, the radial equilibrium equation must take into account radial variations of entropy and enthalpy. In addition, as indicated diagrammatically in Figure 1, radial components of velocity and streamline curvature in the meridional plane will have to be included in the analysis of the flow field at each design station.

In summary, for the stream-filament analysis, the turbine design analysis proceeds along selected streamlines from known inlet conditions with the positions of the streamlines, other than those at the annulus walls, determined from continuity and radial equilibrium considerations. Although one of the objectives of the analysis will be to integrate these individual aspects, it is convenient to review each in turn.

### Analysis Along Streamlines

The basic analysis performed along streamlines will differ little from that which is normally undertaken along the mean line of any axial

turbomachine. In fact, in only two respects can the design procedure be considered different from standard mean-line design practice. Firstly, the radial components of velocity are considered. Secondly, the specific heat at constant pressure,  $c_p$ , of the gas is assumed to vary from station to station through the turbine. The effect on the station-to-station variation of the specific heat is discussed in a later section of the report.

Since the analysis is to form the basis for a computer program, it is convenient to divide the total flow into filaments having equal fractions of the total flow. An odd number of streamlines are selected so that the central streamline can be used as a mean streamline, which serves as the starting point for the solution of the flow field. This mean streamline serves essentially the same function as the mean line in conventional turbine design practice. The radial position of the streamlines at each of the design stations and the streamline values of meridional velocity will in practice be determined from radial equilibrium and continuity considerations. Initially only the boundary streamlines ( $S1$  and  $S5$  of Figure 1) are known, for it is assumed that these follow the specified annulus contours. However, in the following discussion of the streamline equations used in the analysis, it will be assumed that the radial position of all streamlines and their associated meridional velocities are all known quantities.

For the purpose of the current analysis, which is performed in meridional and tangential planes, the absolute velocity vector is defined by two velocity components,  $V_m$  and  $V_u$  and two angles,  $A$  and  $\beta$ . The nomenclature for the flow at a point  $P$  in a streamline surface in an axisymmetric flow in a turbine annulus is illustrated in Figure 2. In terms of



the axial, tangential, and radial velocity components, the analysis variables are defined as follows:

$$\text{Meridional velocity, } V_m = \sqrt{V_x^2 + V_r^2} \quad (1)$$

$$\text{Absolute velocity, } V = \sqrt{V_u^2 + V_m^2} \quad (2)$$

$$\text{Flow angle, } \beta = \tan^{-1} V_u/V_x \quad (3)$$

$$\text{Streamline slope angle, } A = \tan^{-1} V_r/V_x \quad (4)$$

Consequences of the introduction of radial components of flow into the analysis are that the conventional representation of the velocity triangles, which represent the flow on cylindrical surfaces, does not represent the absolute velocities and that the values of station radius may vary from station to station. Sample velocity triangles for the central streamline (S3) shown in Figure 1 are shown in Figure 3 to illustrate the nomenclature. It will be seen that a superscript is used to denote rotor relative flow angles and velocities. Tangential components of velocity are assumed to be negative when opposed to the direction of rotation. Hence, rotor blade relative exit angles have negative values.

As in any design, the calculations performed in the flow direction are to determine the total pressure, total temperature, and the velocity components at each of the design planes; in the streamline analysis these quantities are also to be obtained. However, only the tangential velocities are considered unknown at this time. The evaluation of the meridional velocity is considered later, since its evaluation involves the solution of the flow equations in the meridional plane. In practice, both streamline and meridional plane equations have to be simultaneously

satisfied, but to illustrate the analysis in the streamline direction, it is convenient to consider the solution of the streamline equations as part of an over-all iterative procedure. To a certain extent the developed analysis presented later integrates the two aspects of the solution of the flow field. Nevertheless, the selected over-all procedure still involves an iterative solution of the streamline positions.

The analysis in the streamline direction is illustrated by considering the design stations through a first stage. At inlet to the stage, station 0, the total pressure,  $P_{00}$ , the total temperature,  $T_{00}$ , and the whirl angle,  $\beta_0$ , will all be specified. The remaining quantities of interest at this plane will be determined from the values of meridional velocity obtained from solution of the radial equilibrium and continuity equations. The tangential component of velocity will be given by

$$V_{u0} = V_{m0} \cos A_0 \tan \beta_0 \quad (5)$$

At station 1, the stator exit, the total pressure will be implicitly specified by the row total-pressure-loss coefficient; the total temperature will be equal to the streamline value at the stator inlet; and the tangential velocity will be explicitly specified or the flow angle will be given.

The total-pressure-loss coefficient is defined as follows:

$$\gamma_N = \frac{P_{00} - P_{01}}{P_{01} - P_1} \quad (6)$$

Hence,

$$P_{01} = \frac{P_{00}}{1 + \gamma_N \left(1 - \frac{P_1}{P_{01}}\right)} \quad (7)$$

where

$$\frac{P_i}{P_{o1}} = \left[ 1 - \frac{V_{u1}^2 + V_{m1}^2}{2g_o J c_p T_{o1}} \right]^{\frac{\gamma}{\gamma-1}} \quad (8)$$

Thus, the total pressure,  $P_{o1}$ , can only be obtained when both  $V_{u1}$  and  $V_{m1}$  are known. Since  $V_{m1}$  will be dependent on  $P_{o1}$ , a simultaneous solution for  $P_{o1}$  and  $V_{m1}$  is required.

In preliminary design investigations the tangential velocity will normally be specified, but as a design is finalized, it is convenient to specify the flow angle. In this manner a particular variation of flow angles is obtained directly rather than by an iterative procedure. When the flow angle is specified, the tangential velocity is obtained from the following:

$$V_{u1} = V_{m1} \cos A_1 \tan \beta_1 \quad (9)$$

If  $V_{u1}$  is specified, Equation 9 can, of course, be used to obtain the flow angle.

Thus making the assumption that  $V_{m1}$  will be determined from radial equilibrium and continuity considerations, the stator exit and rotor inlet velocity triangles can be completely defined using standard formulas and techniques.

The next station, 2, is the stage exit. Here again the absolute values of total temperature, total pressure, velocity, and flow angle are considered the principal unknowns. None of these quantities will be directly specified. The total temperature will be obtained from the specified work which is readily expressed in terms of the total temperature drop. Thus,

$$T_{o2} = T_{o1} - \frac{W}{c_p} \quad (10)$$

where  $W$  is the work extracted along the streamline in Btu per lbm.

The tangential velocity component is obtained using the Euler work equation; that is,

$$V_{u2} = \frac{u_1 V_{u1} - g_c J c_p \Delta T_o}{u_2} \quad (11)$$

where  $u_1$  and  $u_2$  are the blade speeds at rotor inlet and exit, respectively.

The stage exit total pressure will normally be obtained from the rotor row total-pressure-loss coefficient,  $\gamma_R$ , but for preliminary analyses it is convenient to specify stage isentropic efficiency,  $\eta_S$  or rotor row isentropic efficiency,  $\eta_R$ . These last two options will avoid the iteration which is involved when the rotor loss coefficient is obtained from a correlation within the computer program. For hand calculations of the velocity triangles, their use considerably reduces the time and effort required to complete a design. Stage exit total pressures are readily obtained from the standard definitions of total-to-total isentropic efficiencies. Thus,

$$P_{o2} = P_{o0} \left[ 1 - \frac{T_{o1} - T_{o2}}{\eta_S T_{o0}} \right]^{\frac{\gamma}{\gamma-1}} \quad (12)$$

or

$$P_{o2} = P_{o1} \left[ 1 - \frac{T_{o1} - T_{o2}}{\eta_R T_{o0}} \right]^{\frac{\gamma}{\gamma-1}} \quad (13)$$

The rotor total-pressure-loss coefficient is defined as

$$\gamma_R = \frac{P'_{o2s} - P'_{o2}}{P'_{o2} - P_2} \quad (14)$$

where  $P'_{02s}$  is the isentropic value of rotor exit relative total pressure. If there is no change in radius of the streamline from rotor inlet to exit,  $P'_{02s}$  will equal  $P'_{01}$ . However, if there is a change of radius, the isentropic relative total pressure is given by the expression

$$\frac{P'_{02s}}{P'_{01}} = \left( \frac{T'_{02}}{T'_{01}} \right)^{\frac{\gamma}{\gamma-1}} = \left[ 1 + \frac{u_2^2 - u_1^2}{2g_0 J c_p T'_{01}} \right]^{\frac{\gamma}{\gamma-1}} \quad (15)$$

Similarly, there is a relationship between the relative exit total pressure and the absolute pressure at stage exit which is readily derived from the velocity triangles using the total-to-static temperature ratios.

$$\frac{P'_{02}}{P_{02}} = \left[ \frac{T'_{02}/T_2}{T_{02}/T_2} \right]^{\frac{\gamma}{\gamma-1}} = \left[ 1 + \frac{u_2(u_2 - 2V_{u2})}{2g_0 J c_p T_{02}} \right]^{\frac{\gamma}{\gamma-1}} \quad (16)$$

Thus, if Equation 14 is reexpressed as

$$\gamma_R = \frac{\left( \frac{P'_{02s}}{P'_{01}} \right) \left( \frac{P_{01}}{P_{02}} \right) \left( \frac{P_{02}}{P'_{02}} \right) - 1}{1 - \left( \frac{P_2}{P_{02}} \right) \left( \frac{P_{02}}{P'_{02}} \right)} \quad (17)$$

and the stage exit static-to-total pressure ratio,  $P_2/P_{02}$ , is expressed in terms of  $V_{u2}$ ,  $V_{m2}$ , and  $T_{02}$ , an explicit expression for  $P_{02}$  can be obtained from Equations 15, 16, and 17 in which  $V_{m2}$  is the only unknown. Hence, as for the stator exit total pressure, the total pressure will have to be obtained from a simultaneous solution of  $P_{02}$  and  $V_{m2}$ .

When  $P_{02}$ ,  $T_{02}$ ,  $V_{u2}$ , and  $V_{m2}$  have been obtained, the stage exit and rotor relative exit velocity triangles are readily obtained using standard turbine design techniques.

In summary, the solution of the streamline flow conditions involve the tangential momentum or work equation and the pressure loss or

energy equation. In the developed form, the analysis uses the differential form of these two basic equations as subsidiary equations in a simultaneous solution of the radial equilibrium equation. The solution of these three equations provides a radial distribution of meridional velocity which satisfies the radial equilibrium requirement and the design specifications. For each station, the meridional velocity distribution is obtained for an assumed value of meridional velocity at the mean streamline. The meridional velocity distribution, however, must also simultaneously satisfy the mass flow continuity conditions.

### The Continuity Equation

The location of the streamlines at each design station and the meridional velocity at each of the streamlines are determined from the mass flow continuity equation. For an axisymmetric flow passing through an axial section of an arbitrary annulus, the continuity equation is as follows:

$$w_T = 2\pi \int_{r_h}^{r_c} \rho V_x r dr \quad (18)$$

where  $w_T$  is the total flow (lbm per sec),  $\rho$  is the static density (lbm per cu ft), and  $r_h$  and  $r_c$  are the hub and casing radii of the station (ft).

Throughout the analysis, total pressure, total temperature, and the tangential and meridional components of the absolute velocity are considered as the principal variables. Hence, it is convenient to reformulate Equation 18 in terms of these variables. Substituting for the density using the standard formula,

$$\rho = \frac{P_0}{RT_0} \left[ 1 - \frac{V^2}{2g_0 J C_P T_0} \right]^{\frac{\gamma}{\gamma-1}} \quad (19)$$

Equation 18 can be reexpressed as follows:

$$w_T = \frac{2\pi}{R} \int_{r_h}^{r_c} \frac{P_0}{T_0} \left[ 1 - \frac{V_u^2 + V_m^2}{2g_0 J C_p T_0} \right]^{\frac{1}{\delta-1}} V_m \cos A r dr \quad (20)$$

Since the radius dependent variables of Equation 20 in general will not be simple analytical functions of radius, the distribution of meridional velocity which satisfies continuity will have to be obtained using an iterative numerical procedure.

When the meridional distribution to satisfy the continuity requirement for the complete annulus flow has been determined, the location of the streamlines which satisfies the continuity requirements of the individual stream filaments must also be computed. For the analysis, streamlines are selected so that any adjacent pair define an annulus containing a preselected constant fraction of the total flow. Thus, it is convenient to introduce a mass flow function  $w(r)$  which varies from zero to unity between the boundary streamlines. This mass flow function is defined as follows:

$$w(r) \equiv \frac{2\pi}{w_T R} \int_{r_h}^r \frac{P_0}{T_0} \left[ 1 - \frac{V_u^2 + V_m^2}{2g_0 J C_p T_0} \right]^{\frac{1}{\delta-1}} V_m \cos A r dr \quad (21)$$

Hence, if the first streamline is at the hub and there are  $n$  streamlines, the  $j^{\text{th}}$  streamline will have a mass flow function value of  $\frac{j-1}{n-1}$ . Thus, the radius of this streamline,  $r_j$ , will be obtained from the solution of the following equation

$$\frac{j-1}{n-1} = \frac{2\pi}{w_T R} \int_{r_h}^{r_j} \frac{P_0}{T_0} \left[ 1 - \frac{V_u^2 + V_m^2}{2g_0 J C_p T_0} \right]^{\frac{1}{\delta-1}} V_m \cos A r dr \quad (22)$$

Thus, streamline positions throughout the flow field can be established once the distribution of meridional velocity has been determined.

This distribution must simultaneously satisfy the continuity and radial equilibrium conditions for the design specification.

### The Radial Equilibrium Equation

A fundamental assumption made in the analysis is that the flow is axisymmetric. Hence, by equating the radial forces acting on a point  $P$  in the flow (see Fig 2), the condition for radial equilibrium is readily shown to be

$$\frac{g_0}{\rho} \cdot \frac{dP}{dr} = \frac{V_u^2}{r} - \frac{V_m^2 \cos A}{r_m} - V_m \frac{dV_m}{dm} \sin A \quad (23)$$

where  $1/r$  and  $1/r_m$  are the tangential and meridional components of streamline curvature, respectively.

The third term on the right-hand side of Equation 23 results from a change in momentum in the meridional direction. However, in general, the change in both meridional velocity in the interblade row space and the sine of the streamline slope will be small. Hence, for the turbine design analysis, this third term will be assumed to be negligibly small. If it were decided that this term should be included in the analysis, it would be necessary to extend the analysis to consider the complete flow field defined by the trailing and leading edges of the upstream and downstream blade rows and the annulus walls rather than a section of the flow field on an axial plane. Thus, it would be necessary to make the assumption that the flow was axisymmetric at blade leading and trailing edges, which is considerably less valid than that concerning the axial symmetry at an interblade row design station.

Omitting the third term on the right-hand side, Equation 23 simplifies to



$$\frac{g_0}{g} \cdot \frac{dP}{dr} = \frac{V_u^2}{r} - \frac{V_m^2 \cos A}{r_m} \quad (24)$$

This is the fundamental radial equilibrium equation used in the current analysis. The use of Equation 24 rather than Equation 23 simplifies the problem of solution considerably. However, the streamline slope and curvature in the meridional plane,  $A$  and  $1/r_m$ , still necessitate consideration of derivatives with respect to the axial direction,  $X$ . That is,

$$A = \tan^{-1} \left( \frac{dr}{dx} \right) \quad (25)$$

and

$$1/r_m = \frac{d^2r/dx^2}{[1 + (dr/dx)^2]^{3/2}} \quad (26)$$

Hence, the radial equilibrium equation contains derivatives with respect to both  $r$  and  $X$ . If the analysis were to be performed for an axisymmetric flow in an arbitrary duct, it could readily be extended to consider the path of individual streamlines in the meridional plane. However, in a turbine design-point analysis, it is unrealistic to assume that the axisymmetric form of the radial equilibrium equation can be extended beyond the interblade row space into the blade rows. Thus, the boundary conditions for the meridional streamlines in the interblade row space are indeterminate at the trailing edge and leading edge planes defining this space. Only the boundary streamlines, at the inner and outer annulus walls, are rigorously defined--by the assumption that these streamlines follow the contours of the annulus wall. In the absence of a rigorous analytical treatment for the slope and curvature of the flow in the meridional plane, it becomes necessary to adopt an arbitrary solution to the problem. In

the current analysis, streamline slope and curvature in the meridional plane will be treated in one of two ways:

- a. The slope and curvature of the boundary streamlines will be obtained from a definition of the wall contours, and then both  $A$  and  $1/r_m$  will be assumed to be linear functions of radius determined from values at the walls.
- b. The slope and curvature will both be specified arbitrarily as a function of radius.

It is appreciated that other arbitrary solutions are possible. For example, existing design and off-design analyses developed at NREC and elsewhere for axial and centrifugal compressors have evaluated the slope and curvature of intermediate streamlines by spline-fitting curves, representing these streamlines, through points at the design stations. For turbine design, however, it would be difficult to justify the increased complexity of the analysis, particularly when the influence of the blading on the streamline flow through the row is not considered. The radial and axial distribution of loading and blade blockage throughout the rows will undoubtedly have a larger influence on the values of  $A$  and  $1/r_m$  at a selected design station than the distribution of the flow at adjacent design stations.

With the incorporation of the assumption that slope and curvature are functions of radius, the radial equilibrium equation is of the form,

$$\frac{g_0}{\rho} \cdot \frac{dP}{dr} = \frac{V_u^2}{r} - V_m^2 f(r) \quad (27)$$

Hence, the radial equilibrium equation can be solved station by station

throughout a turbine without an iterative procedure which involves other stations. The solution will depend only on the specified design requirements, the preceding row losses, and the flow conditions at the preceding design station, and not on any data concerning the flow at subsequent design stations.

Since the continuity equation and the subsidiary streamline equations have all been expressed in terms of the turbine design variables of total pressure, total temperature, and the velocity components, it is convenient to express the radial equilibrium equation in terms of these variables. Thus, it is necessary to reexpress the density and static pressure. The appropriate substitution for density has been presented earlier as Equation 19; the static pressure,  $P$ , is given by the standard relationship

$$P = P_o \left[ 1 - \frac{V_u^2 + V_m^2}{2g_o J c_p T_o} \right]^{\frac{\gamma}{\gamma-1}} \quad (28)$$

Hence, from Equation 19 and the differentiation of Equation 28, Equation 27 can be reexpressed as follows:

$$\begin{aligned} \frac{V_u^2 + V_m^2}{2} \cdot \frac{1}{T_o} \frac{dT_o}{dr} - V_u \frac{dV_u}{dr} - \frac{1}{2} \frac{dV_m^2}{dr} + g_o R T_o \left[ 1 - \frac{V_u^2 + V_m^2}{2g_o J c_p T_o} \right] \frac{1}{P_o} \frac{dP_o}{dr} \\ = \frac{V_u^2}{r} - \frac{V_m^2 \cos A}{r_m} \end{aligned} \quad (29)$$

Since the radial equilibrium equation has to be solved simultaneously with two basic streamline equations (the tangential-momentum equation and the total-pressure-loss equation), the principal analysis variables are considered to be  $\frac{dV_m^2}{dr}$ ,  $\frac{1}{P_o} \frac{dP_o}{dr}$ , and  $\frac{dV_u}{dr}$ . Therefore, for its subsequent solution, Equation 29 is rewritten as

$$C_{11} \frac{dV_m^2}{dr} + C_{12} \frac{1}{P_0} \cdot \frac{dP_0}{dr} + C_{13} \frac{dV_u}{dr} = C_{14} \quad (30)$$

where  $C_{11}$ ,  $C_{12}$ ,  $C_{13}$ , and  $C_{14}$  are coefficients which are readily obtained from the design specifications. It can be readily seen from Equation 29 that  $C_{11}$  can be set equal to unity,  $C_{13}$  equal to  $2V_u$  and that the remaining coefficients will then be given by

$$C_{12} = \frac{R}{J C_p} [V_u^2 + V_m^2 - 2g_0 J C_p T_0] = \left(\frac{\gamma-1}{\gamma}\right) [V_u^2 + V_m^2 - 2g_0 J C_p T_0] \quad (31)$$

and

$$C_{14} = (V_u^2 + V_m^2) \frac{1}{T_0} \cdot \frac{dT_0}{dr} - \frac{2V_u^2}{r} + \frac{2V_m^2 \cos A}{r_m} \quad (32)$$

The development of the analysis, which consists essentially of establishing a calculational procedure for the solution of the flow field at each design plane is discussed later. It will be shown that the two basic equations governing the flow in the streamline direction can be expressed as differential equations having the same form as Equation 30.

It will be noted that in deriving the particular form of the radial equilibrium equation to be used in the computer program solution of the flow field, it was assumed that the specific heat and the specific heat ratio,  $C_p$  and  $\gamma$ , are independent of radius. Similarly, throughout the discussion of the streamline equations it was implicitly assumed that these gas properties were known constants. For the analysis it will be assumed that the specific heat will be constant at any axial station but may be specified to vary through the turbine.

## MODIFICATIONS TO THE STREAM-FILAMENT APPROACH FOR VARYING SPECIFIC HEAT, MIXING, AND COOLANT FLOWS

### Introduction

In the preceding section of this report in deriving the stream-line equations, it was assumed that the specific heat was constant. However, the analysis is to form the basis for a computer program to be used for multistage and multispool turbine configurations. Thus, in many design investigations the variation in temperature through the machine will be sufficiently large that the variation of specific heat will be a significant factor. The analysis will be modified to accommodate a station-to-station variation of specific heat, and these modifications are presented in this chapter.

The stream-filament approach assumes the flow field to consist of concentric surfaces of revolutions defined by selected streamlines. In an actual turbine it is unrealistic to assume that there will not be any mass transfer between these stream filaments. While the flow, which remains in the free stream throughout its passage through a turbine, will probably remain within its original filament, the flow which is affected by the viscous forces near blade surfaces will tend to migrate to other filaments under the influence of the complex static pressure field which is set up within a turbine. Experimental test data from turbine stages suggest that for many turbines this mixing is sufficiently severe that the basic stream-filament approach should be capable of modification to represent, at least qualitatively, this mixing.

An additional factor which must be considered in many turbine applications is the addition of coolant flows to the main stream. Coolant flows can be added to the main stream in a variety of ways. For example,

disk and rotor root coolant flow will enter along the hub contour, rotor convective cooling flows will normally enter the main stream at the outer casing, and where film or transpiration cooling is used, the coolant flow will be distributed across the annulus. Irrespective of the manner of admission, the principal effects which should be considered in any modification of the fundamental stream-filament approach will be to increase the flow and to change the temperature level of the main stream. The modifications which are made to accommodate a specified coolant schedule in the analysis are discussed in the last section of this chapter.

#### Variations of Specific Heat

The simultaneous solution of the radial equilibrium and continuity equations at the turbine design stations is considerably simplified by the assumption of a radially constant value of specific heat. Using the standard formulas for total-to-static temperature and pressure ratios, which assume a constant specific heat, the form of these two basic equations are amenable to solution in terms of the principal variables  $P_o$ ,  $T_o$ ,  $V_u$ , and  $V_m$ . Thus, the principal justification for the use of radially constant specific heat and specific heat ratio must be that it considerably simplifies the numerical solution of the radial equilibrium and continuity equations. However, it should be noted that at a stator exit station of a design in which there is a zero reaction at the stator casing section and zero reaction at the following rotor hub section, the radial variation of specific heat will be as large as that which exists across a stage.

When two or more design stations of differing specific heat are used in the foundation of the streamline equations, an appropriate mean value of specific heat will be used. The work, blade row loss, and

isentropic efficiency expressions all involve conditions at two stations. When the specific heat is not assumed to be constant, the Euler work equation has to be expressed as

$$h_{01} - h_{02} = \int_2^1 c_p dT_0 = \frac{u_1 V_{u1} - u_2 V_{u2}}{g_c J} \quad (33)$$

The integral  $\int_2^1 c_p dT_0$  will be approximated as follows:

$$\int_2^1 c_p dT_0 \cong \bar{c}_p (T_{01} - T_{02}) \quad (34)$$

where

$$\bar{c}_p \equiv \frac{c_{p1} + c_{p2}}{2}$$

Similarly when the equations involve an isentropic expansion from one station to another, the expansion index will be based on a mean value of specific heat. Thus, for a stage pressure ratio,  $P_{00}/P_{02}$ , the isentropic temperature ratio will be defined as

$$\frac{T_{00}}{T_{02s}} = \left( \frac{P_{00}}{P_{02}} \right)^{(\gamma_s - 1)/\gamma_s} \quad (35)$$

where

$$\frac{\gamma_s - 1}{\gamma_s} \equiv \frac{R}{J} \frac{2}{c_{p0} + c_{p2}}$$

The approach of using an appropriate mean value of the specific heat when the thermodynamic relationship relates state conditions at differing stations will lead to more complex expressions for all the streamline equations. For example, the stage efficiency equation will contain three specified values of specific heat. That is,

$$\eta_s = \frac{(c_{p1} + c_{p2})(T_{01} - T_{02})}{T_{00} \left[ 1 - \left( \frac{P_{02}}{P_{00}} \right)^{2/\gamma_s (c_{p0} + c_{p2})} \right] (c_{p0} + c_{p2})} \quad (36)$$

For a single stage the actual variation between  $C_{p0}$ ,  $C_{p1}$ , and  $C_{p2}$  will be relatively small, and the calculated efficiency will differ little from a value obtained from a design in which a constant specific heat has been assumed. In a multistage unit, the over-all variation in  $C_p$  may be more significant. Thus, it could be argued that the ideal work should be based on individual stage isentropic temperature drops calculated from the appropriate stage values of pressure ratio, stage mean specific heat, and inlet total temperature. However, the isentropic temperature drop for the complete spool, which will be used in the expression for over-all efficiency, will be simply obtained from the over-all pressure ratio, the spool inlet total temperature, and a mean specific heat ratio for the spool.

### Mixing

In the current analysis, no attempt is made to accurately represent the complex viscous flow phenomena which occur in a turbine, nor to assign any loss in blade row efficiency to the interfilament mixing process. Experimental investigations using flow visualization techniques and the detailed analysis of turbine performance using data from radial and circumferential surveys clearly show that mixing can be sufficiently severe that the fundamental streamline analysis should be modified to represent at least qualitatively the mass flow mixing which occurs between the axisymmetric stream filaments.

While secondary flows have associated losses, and one of the mixing mechanisms is undoubtedly these secondary flows, the correlation of losses to be used in the design analysis program has loss levels which are in excess of those due to profile loss. Hence, for the purpose of



this analysis, no loss is assumed to be directly associated with mixing. Thus, if a total pressure or total temperature profile is modified, the new profiles will have the original mass flow weighted values. This consideration leads to a formulation of a mixing model of the following form:

$$P_{0j}^* = (1 - x_j) P_{0j} + x_j \frac{\sum_R x_R \Delta w_R P_{0R}}{\sum_R x_R \Delta w_R} \quad (37)$$

and

$$T_{0j}^* = (1 - x_j) T_{0j} + x_j \frac{\sum_R x_R \Delta w_R T_{0R}}{\sum_R x_R \Delta w_R} \quad (38)$$

where  $P_{0j}^*$  and  $T_{0j}^*$  are the mixed values of total pressure and total temperature for streamline  $j$ . The mixing parameter,  $x_j$ , can be specified for individual streamlines, but the same value will be used for both total pressure and total temperature. Since the  $n$  streamlines will define  $(n-1)$  stream filaments of equal flow, the flow associated with individual streamlines,  $\Delta w_k$ , will equal  $\frac{w}{(n-1)}$  for internal streamlines and  $\frac{w}{2(n-1)}$  for the hub and casing boundary streamlines. Both equations satisfy the set requirement that the mass flow weighted mean values of mixed and unmixed profiles will be equal. With the above formulation for mixing, any radial distribution of the streamline mixing factor may be specified with the exception of those for which  $\sum x_k \Delta w_k = 0$ . No mixing is, of course, one of these special cases, but then it will be unnecessary to use Equations 37 and 38 since the streamline values of total pressure and temperature will be unmodified. If experimental data indicate that complete mixing occurs near the annulus walls but that virtually no mixing occurs in the central portion of the annulus, the appropriate streamlines could be assigned values of 1.0 and 0.0, respectively.

Even though the mixing parameter has been selected as a streamline dependent variable, it can, of course, be specified as a constant for

a particular row. In these circumstances, Equations 37 and 38 simplify to become

$$P_{oj}^* = (1-x) P_{oj} + x \cdot \bar{P}_o \quad (39)$$

and

$$T_{oj}^* = (1-x) T_{oj} + x \cdot \bar{T}_o \quad (40)$$

where  $\bar{P}_o$  and  $\bar{T}_o$  are mass flow weighted values for the original profiles.

In many analyses it is probable that constant values of  $X$  will be specified. For a fully mixed solution with  $X=1.0$  at each streamline, the mixed values would equal the corresponding mass flow weighted value.

Having chosen a mathematical formulation for the mixing, it is necessary to decide at what point it is to be introduced into the analysis. Since mixing is related to the flow within a blade row, it would appear logical to specify mixing parameters for blade rows rather than design stations. Thus, the mixing will occur before or after the design stations at which radial equilibrium and continuity equations are satisfied. The modification from streamline to mixed values of absolute total pressure and total temperature will be made downstream of the plane at which radial equilibrium and continuity equations are satisfied and will be used as inlet values for the following blade row in which mixing is assumed to occur. Thus, revised values of inlet total pressures will be used in the total-pressure-loss coefficient expression, and the revised values of inlet total temperature will be used as the datum for the temperature drop through the rotor row. The selection of the row inlet rather than the row exit plane considerably simplifies the numerical calculations at the following interrow design station where radial equilibrium

and continuity are again satisfied.

Since the mass flow weighted values of the revised total pressures and total temperatures will be unchanged from the corresponding stream-filament values, the stage mean values of efficiency and work output will not be directly affected by specified mixing. Some small effects on mass flow weighted stage efficiency is to be expected, since the levels of loss coefficient will be dependent on the computed blade geometries. The distribution of flow angles and velocities will, of course, depend on the solution of the radial equilibrium and continuity equations at the following design station, and hence the modification of the radial gradients of enthalpy and entropy due to mixing will have some effect on the levels of loss. Unfortunately, it will be necessary to develop the computer program before the influence of mixing can be fully investigated. Nevertheless, it is clear that significant effects are to be expected if large gradients of total pressure and total temperature (which result from the computed radial distributions of loss coefficients and specified work extraction) are assumed to fully mix. Since some of the total pressures used in the total-pressure-loss equation will be greater than their corresponding unmixed values, it is quite possible that stream-filament efficiencies, based on mixed values of total pressure and total temperature will be in excess of 100 per cent in some instances. Such anomalies have been observed experimentally in turbine stages tested with a radial distribution of stage inlet total temperature. In order to provide guidance to the program user on the effects of the specified mixing, both the streamline and mixed values of total pressure and total temperature will be included in the computer program output. It should be emphasized however that the particular values of the mixing parameter which

will be specified for a selected turbine design-point analysis will have to be fully investigated using the computer program as an analytical tool in conjunction with detailed experimental data for similar turbines at a later date.

### Coolant Flows

For some high inlet temperature turbines, the amount of coolant mass flow admitted to the main stream will be sufficiently large that significant mismatching of stages would result if the coolant mass flow schedule were not an integral part of the design-point analysis. The temperature level of the coolant must also be considered. The relevant temperature is, of course, the initial temperature of the coolant which will often be that of the compressor delivery air. Even though at the point of admission the coolant flow, which has been used for blade cooling may be close to the temperature of the main stream, it will have attained this temperature because heat has been transferred from the main stream by way of the blading. Hence, the local temperatures to be used in the design-point analysis should be derived from consideration of the heat balance equation. Thus, coolant mass flows and temperatures will have to be specified for the design-point analysis of a cooled turbine. However, since the coolant may be admitted in a number of ways, it is inappropriate to consider the pressure level of the coolant, its flow direction, or its radial distribution in a general design-point analysis. Similarly, any losses associated with the introduction of coolant cannot readily be accommodated within a stream-filament analysis other than by the program user directly specifying row loss coefficients or additional loss factors for the rows whose performance will be affected by the coolant.

As with the mixing previously discussed, the addition of coolant will be considered as a blade row rather than an interblade row process. Hence, the coolant flow schedule will be specified in terms of the mass flow and temperature of the coolant for each of the cooled rows. The treatment of the two aspects of the coolant flow is discussed, in turn.

Considering the coolant mass flow which is added to the main stream in the blade row which precedes design station  $n$ , the continuity equation for this station will be written as

$$\dot{w}_n = \dot{w}_{n-1} + \Delta \dot{w} = 2\pi \int_{r_h}^{r_c} \rho V_x r dr \quad (41)$$

where  $\Delta \dot{w}$  is the coolant flow added to the main stream in the blade row preceding station  $n$ .

In the calculation of the gas temperatures resulting from the addition of coolant to the main stream, it will be assumed that the coolant will be uniformly distributed between the main stream filaments. Hence, the temperatures will be modified on a streamline basis with the new temperature,  $T_{0j}^{**}$ , of the  $j^{\text{th}}$  streamline being given by the expression

$$T_{0j}^{**} = \frac{\dot{w}_{n-1} T_{0j} + \Delta \dot{w} T_{0c}}{\dot{w}_{n-1} + \Delta \dot{w}} \quad (42)$$

With the addition of cooling being considered a blade row phenomenon, the change in temperature is assumed to occur between design stations. As with the mixing previously discussed, a decision has to be made whether to make the temperature level correct at a blade leading edge plane (which is immediately downstream of a design axial station) or

at a trailing edge plane (immediately upstream of the next design station at which radial equilibrium and continuity are to be satisfied). For stator blading, where streamline total temperatures are constant through the row, the final temperatures would be identical for the two alternative methods. For the rotor, across which there is a change in absolute total temperature level, there will be small differences between the results of the two methods because the radial gradient of temperature will be changed in any design where radial variations of work output has been specified. However, the numerical solution of the design problem and construction of the computer program are simplified by correcting the temperature level at the inlet plane of a cooled row; this approach has been selected.

For a stage in which coolant is added to the main stream in either or both of the blade rows, there is no generally accepted definition of the stage isentropic efficiency; the expansion process is, in fact, no longer isentropic even in the absence of losses. For the current analysis it is assumed that all the flow which leaves the stage contributes to the work output of that stage. Thus, if station  $n$  is a stage exit, the stage total temperature drop,  $\Delta T_o$ , along any selected streamline is obtained from the specified total power output (in Btu's) and distribution of output and the total flow,  $w_n$ . That is,

$$\Delta T_o = T_{oj_{n-1}}^{**} - T_{oj_n} = \left[ \frac{P}{w_n C_{PR}} \right]_j \quad (43)$$

The total temperature  $T_{oj}^{**}$  is obtained by correcting the stage inlet total temperature for both the stator and rotor coolant flows,  $\Delta w_N + \Delta w_R$  where

$$W_n = W_{n-2} + \Delta W_N + \Delta W_R \quad (44)$$

It will be assumed that the ideal power output of the stage is that available from the expansion of both the main flow and the coolant flows across the stage pressure ratio. That is,

$$P_s = C_{p_s} \left[ 1 - \left( \frac{P_{0N}}{P_{0n-2}} \right)^{\frac{\gamma_s-1}{\gamma_s}} \right] \left\{ W_{n-2} T_{0n-2} + \Delta W_N T_{0N} + \Delta W_R T_{0R} \right\} \quad (45)$$

From Equations 43 and 45 the expression for stage efficiency becomes

$$\eta = \frac{C_{p_R} (T_{0n-1}^{**} - T_{0R})}{C_{p_s} \left\{ 1 - \left( \frac{P_{0N}}{P_{0n-2}} \right)^{\frac{\gamma_s-1}{\gamma_s}} \right\} T_{0n-1}^{**}} \quad (46)$$

where

$$T_{0n-1}^{**} = \frac{W_{n-2} T_{0n-2} + \Delta W_N T_{0N} + \Delta W_R T_{0R}}{W_{n-2} + \Delta W_N + \Delta W_R}$$

The over-all efficiency of a spool having cooled stages will be expressed as a summation of actual power outputs divided by a summation of ideal power outputs. The summation of actual power outputs is, of course, directly obtained from the design specifications; the ideal power output of the turbine inlet flow and that of the individual stage coolant flows will be evaluated using the appropriate values of pressure ratio and inlet total temperature.

### Concluding Remarks

Relatively simple modifications to the constant specific heat stream-filament analysis are used to take account of variations of specific heat, interfilament mixing, and the addition of coolant flows.

There are two principal justifications for the use of relatively simple models. Firstly, they are readily accommodated within the structure of a purely stream-filament analysis. Secondly, for the majority of applications the effects will be relatively unimportant. For many single or two stage turbines the actual variation of specific heat will be almost insignificant. Although the effects of interfilament mixing cannot, at this time, be fully investigated, it would appear probable that only for designs in which large gradients of work extraction are specified will the total pressure and total temperature profiles be greatly changed by mixing effects; however, experience with stream-filament designs indicate that if too severe a radial gradient of work extraction is specified, the blading geometries become mechanically unacceptable or it becomes impossible to satisfy the requirement of radial equilibrium. Total coolant flows will, in general, be a relatively small percentage of the machine inlet flow and in multistage applications will be limited to the early blade rows; while the model for the addition of coolant to a particular stage is relatively simple and open to question, the correction to the levels of flow and temperature for the calculation of the geometry of the downstream stages will be valid. The avoidance of stage mismatching is the most important aspect of cooled turbine designs, and this is adequately considered in the proposed model.

While mixing will invalidate the concept of a stream-filament efficiency, the mass flow weighted stage efficiencies will not be directly affected in the mixing. All efficiencies will be influenced by the introduction of coolant. While the selected definitions of efficiency for cooled stages are not necessarily generally accepted, the



program output will contain all the total pressures and temperatures generated in the design-point analysis; from these data, alternatively defined efficiencies may be readily obtained.

## DEVELOPMENT OF THE LOSS CORRELATION

### Introduction

It is self-evident that the most sophisticated numerical analysis of a selected turbine design requirement would be of little value if blade row performance data used in conjunction with the analysis were not consistent with the blading to be used for the design. In adopting a stream-filament approach to turbine design, the loss data required are for elements of blading in a stage environment and as such are not readily available. Simple cascade data can provide a guide to the expected performance, but profile loss is often a relatively small percentage of the total loss. Apart from the basic question of loss level, cascade data are frequently presented in terms of the over-all profile geometry such as blade angles, solidity, and thickness/chord ratio but are rarely related to the detailed design of the profile; the latter is undoubtedly a significant factor, since it ultimately governs the growth of boundary layers. For a design-point analysis, it is desirable to relate loss levels to the design requirements which can be expressed in terms of the over-all loading of the section required by the design. A basic assumption made in the present analysis is that the blading is suitably designed to avoid the excessive losses associated with unsuitable profiles, solidities, or incidence settings. Since every turbine is a compromise between aerodynamic and mechanical requirements, it is inevitable that blade row losses are often increased as a result of mechanical requirements. Hence, the datum level of loss which is to be an integral part of the computer program must in some instances be factored to compensate for any anticipated increase in loss.

Since there is little available data on which to base element losses, the present loss correlation was obtained from a correlation of achievable stage efficiencies. The manner in which the correlation was obtained and some checks on the validity of the correlation are presented in the following sections. Loss factors and kinetic-energy-loss coefficients are also briefly discussed.

#### Data for the Loss Correlation

Since the loss coefficient data are to be applied along streamlines passing through blade rows, it would appear that the correlation should be based on experimental traverse data from turbine stage tests. Unfortunately, very few detailed radial traverse investigations are undertaken during turbine stage performance testing and even less data are readily available in the published literature. Hence, it is necessary to base the correlation on over-all stage results using the frequently adopted mean-line approach to turbine analysis. While considerably more data exist for complete stage designs, it is important that these data reflect what is achievable in terms of efficiency level rather than that which is measured when a design is inefficiently bladed or is operating at off-design conditions.

The principal source of data used for the correlation is the stage efficiency correlation of Reference 1. This reference contains a contour plot of achievable stage efficiencies correlated against the over-all stage design parameters of stage loading factor,  $y_o J c_p \Delta T_o / u^2$ , and stage flow factor,  $V_x / u$ . This particular plot, which is based on the results from a large number of turbine stage performance tests, is reproduced as Figure 4. The efficiency levels shown are corrected to

remove that loss which is believed to be due to tip clearance effects. In general, the shape of the contours and levels of efficiency shown in the correlation of Reference 1 differs little from similar correlations obtained by other aircraft gas turbine manufacturers. The stage loading factor and stage flow factor do not uniquely define the turbine design velocity triangles but by making four assumptions, the stage performance correlation can be used as a source of individual row total-pressure-loss coefficients.

These assumptions are:

1. Rotor and stator loss coefficients will be equal when their relative design requirements are identical.
2. The turbines presented in the correlation were designed with 50 per cent stage reaction at the mean line.
3. The axial velocity is constant through the stage.
4. The stator exit Mach numbers were 0.8.

Each of these assumptions is considered in turn.

The first assumption is a fundamental requirement of a stream-filament analysis; one of the basic requirements of the correlation is that it can be used for any design section irrespective of whether it is a rotor or stator row and its radial location in the annulus. In the event that use of the analysis program, in conjunction with test results from turbine stages designed using the stream-filament method, provides basic data which do not support this assumption, loss correction factors will have to be employed to adjust loss levels.

The second assumption is expected to be valid. The majority of turbines used in the correlation will have mean section stage reactions (defined as the ratio of static temperature drop across the rotor to the

stage total temperature drop expressed as a percentage) in the range from 40 to 60 per cent. Even though the stages may not in every case have a 50 per cent stage reaction, the effect on efficiency level of any small difference from 50 per cent is likely to be small. Although not a necessary assumption for the derivation of row loss data, it is of interest to note that the majority of turbines used in the correlation would have had rotor hub-section reactions sufficiently far from impulse conditions that the stage efficiency levels would not be greatly affected.

From published engine information, it is evident that the turbine stages used in the correlation were designed with significant amounts of annulus flare, and from this it can be concluded that many of the designs will closely approximate constant axial velocity designs. Hence, the third assumption is reasonable.

The actual Mach number levels for the stages tested are unknown, but it is extremely likely that the assumption of a stator exit value of 0.8 is reasonably valid; deriving stage pressure ratios for the selected velocity triangles shows these lie in the range 1.5 to 2.0:1, which is the range of stage pressure ratio likely to be used in aircraft engine applications.

With these four assumptions, complete velocity diagrams may be obtained for any turbine design point which is defined in terms of its stage loading factor,  $\psi = \frac{g_0 J C_p \Delta T_0}{u^2}$ , and stage flow factor,  $\phi = \frac{V_x}{u}$ . Hence, using efficiencies from Figure 4, it is possible to deduce the row total pressure loss coefficients of selected turbine designs. From the definition of reaction

$$\bar{R} = \frac{T_1 - T_2}{T_{00} - T_{02}} = 1 + \frac{\kappa}{2} - \frac{V_{u1}}{u} \quad (47)$$

the ratio  $V_{u1}/u$  is obtained. Hence, the stator exit angle  $\beta_1$ , is readily computed from the expression

$$\beta_1 = \tan^{-1} \left\{ \frac{V_{u1}/u}{V_{x1}/u} \right\} = \tan^{-1} \left\{ \frac{0.5 + \psi/2}{\phi} \right\} \quad (48)$$

The relative flow angle,  $\beta_1'$ , is given by the equation

$$\beta_1' = \tan^{-1} \left\{ \frac{\psi/2 - 0.5}{\phi} \right\} \quad (49)$$

With the angles of the stator exit and rotor relative inlet diagrams defined by selected values of  $\psi$  and  $\phi$ , these diagrams can be completed in terms of the velocity parameters ( $\frac{V_1}{\sqrt{T_{01}}}$ ,  $\frac{u}{\sqrt{T_{01}}}$ , etc.) by assigning a value to the stator exit Mach number.

The assumptions of 50 per cent reaction and constant axial velocity across the rotor produce stage exit and rotor relative exit diagrams which are similar to those at stator exit; that is,  $\beta_2 = -\beta_1'$  and  $\beta_2' = -\beta_1$ . To completely define these stage exit velocity triangles, the ratio of stage exit to inlet total temperature,  $T_{02}/T_{00}$ , is required and this ratio is simply obtained from the definition of stage loading factor. That is,

$$\frac{T_{02}}{T_{00}} = 1 - \frac{\psi}{g_0 J c_p} \left( \frac{u}{\sqrt{T_{01}}} \right)^2 \quad (50)$$

Thus, all the relevant velocity parameters can be computed using the blade speed parameter at stage exit  $\frac{u}{\sqrt{T_{02}}}$  where  $T_{01} = T_{00}$  and

$$\frac{u}{\sqrt{T_{02}}} = \frac{u}{\sqrt{T_{01}}} \sqrt{\frac{T_{00}}{T_{02}}} \quad (51)$$

In addition to the normally computed velocity triangle quantities, the stator exit absolute and rotor exit relative values of total-to-static pressure ratios,  $P_{01}/P_1$  and  $P_{02}'/P_2$ , are also required in order

to derive row total pressure loss coefficients. The relationship between stage isentropic efficiency,  $\eta_s$ , and row loss coefficients,  $\gamma_N$  and  $\gamma_R$ , is as follows:

$$\frac{1}{\eta_s} = 1 + \frac{T_{02}}{\Delta T_0} \left( \frac{\gamma-1}{\gamma} \right) \left\{ \gamma_N \left( 1 - \frac{P_1}{P_{01}} \right) + \gamma_R \left( 1 - \frac{P_2}{P_{02}} \right) \right\} \quad (52)$$

The above expression is an approximation, but it is of a high order of accuracy when the efficiency level is in excess of 85 per cent. Using the appropriate values of efficiency obtained from Figure 4 for the selected design points, Equation 52 can be solved for the rotor loss coefficient,  $\gamma_R$ , provided the stator loss coefficient,  $\gamma_N$ , is also known. Values of  $\gamma_N$  are obtained from design points having a unity stage loading factor; for these turbines the rotor inlet angle is zero (see Equation 49) and the two row loss coefficients are assumed to be equal, making it possible to evaluate them from Equation 52.

The loss data used for the correlation are based on four stator configurations, these having exit angles of 71.8, 60, 51.3, and 45 degrees. Additional data points were obtained for various rotor blades by considering design points having these stator exit angles. These design points lie on four straight lines in the  $\gamma \sim \phi$  diagram. The equations of these lines are obtained from Equation 48, which can be reexpressed as

$$\frac{\gamma}{2} = K\phi - 0.5 \quad (53)$$

where the constant  $K$  of any selected line is equal to the tangent of the stator exit angle,  $\tan \beta_1$ . The loss coefficient correlation is based on 18 design points that span the area of the efficiency correlation which is substantiated by measured turbine performance. (Turbine test data points have been omitted from Figure 4 but are shown in the corresponding

figure of Reference 1.)

### Correlation of Total-Pressure-Loss Coefficients

One of the widely used correlations (that due to Soderberg) assumes loss is principally a function of deflection. Hence, one of the first correlations attempted was total-pressure-loss coefficient versus row deflection shown in Figure 5. Points having the same exit angle are joined by lines in this figure, and values of row reaction are noted against individual points. It will be seen that loss coefficients generally increase with deflection but that row reaction has a strong influence on the level. The same data points are replotted in Figure 6 using row reaction as the abscissa. (Row reaction is defined as  $(1 - V_{in}/V_{ex})$  where  $V_{in}$  and  $V_{ex}$  are the inlet and exit velocities relative to the blade section.) In Figure 6 the values of deflection are noted against the points. Assuming row deflection,  $\delta$ , and row velocity ratio,  $\frac{V_{in}}{V_{ex}}$ , are the relevant parameters, the data are correlated to a reasonable degree of accuracy by the following expression:

$$Y = (0.0007\delta + 0.00005\delta^2) \left\{ 3 - 9 \left( \frac{V_{in}}{V_{ex}} \right) + 10 \left( \frac{V_{in}}{V_{ex}} \right)^2 \right\} \quad (54)$$

where  $\delta$  is the row deflection in degrees.

While the above correlation reproduces the efficiency contours of Figure 4 with acceptable accuracy, it cannot be considered acceptable from theoretical considerations. The above correlation implies that when the velocity ratio,  $\frac{V_{in}}{V_{ex}}$ , falls below 0.45, the level of loss for a selected deflection begins to increase. This result is unacceptable, since it is to be expected that losses will decrease smoothly as the over-all row acceleration increases at a constant deflection. The high reaction blading,



with low values of  $V_{in}/V_{ex}$  will have high values of exit angle. Hence, the possibility that the increase in loss was due to trailing edge blockage effects was investigated. In Figure 7 the loss coefficient data were replotted with blade row exit angle as the abscissa. Even though the indications are that a theoretically acceptable variation of loss with reaction could be obtained if the exit angle were introduced as a parameter in the correlation, the over-all correlation would be complex.

In the initial correlation, the inlet and exit angles appear together as deflection; a review of the basic data showed that the unacceptable form of the reaction factor could be traced to a failure to distinguish between blades having the same deflection but significantly different design requirements. For example, in Figure 6 a 70 degree deflection can be located on the three curves having exit angles of 51.3, 60, and 71.8 degrees. The inlet angles corresponding to 70 degree deflections are 18.7, 10, and -1.8 degrees, and the row reactions are 0.34, 0.49, and 0.69, respectively. It will be seen that the loss coefficients of the first and last are greater than that of the intermediate blade. The use of deflection as a correlating parameter is clearly the reason for the theoretically unsound dependence on velocity ratio given in Equation 54. The basic difference between the three profiles considered in the above example is the change in angular momentum that is required of the profiles. The tangential loading of the profile is directly related to the change in tangential velocity across the row, and hence it is logical to consider tangents of the inlet and exit angles rather than the actual angles in the correlation.

If the inlet and exit axial velocities are assumed to be equal,

the change in tangential velocity is proportional to  $-\tan\beta_{in} + \tan\beta_{ex}$  for stators and  $\tan\beta_{in} - \tan\beta_{ex}$  for rotors. Thus,  $|\tan\beta_{in} - \tan\beta_{ex}|$  can be selected as a tangential loading function. To investigate a possible correlation of the form

$$Y = |\tan\beta_{in} - \tan\beta_{ex}| f\left(\frac{V_{in}}{V_{ex}}\right) \quad (55)$$

loss coefficients were divided by their tangent function and plotted against the row velocity ratio (see Fig 8). It will be seen that the dependence of loss level on the velocity ratio is now of the expected form, with loss level increasing as the design requirement approaches impulse conditions,  $V_{in}/V_{ex} = 1.0$ . There would appear to be some dependence on exit angle which again indicates the possibility that trailing edge blockage might be a factor in the level of loss. Since blade trailing edge thicknesses are frequently selected to be a constant fraction of the blade pitch or chord, it might be expected that trailing edge loss would increase with trailing edge exit angle. The trailing edge blockage is represented by the ratio of trailing edge thickness to the exit flow area,  $t_{te}/(S \cos\beta_{ex})$ . Hence, if the ratio  $t_{te}/S$  is approximately constant for standard blade design practice, the level of loss might be expected to be a function of  $\cos\beta_{ex}$ . Based on the loss data, a correlation of the type

$$Y = \frac{|\tan\beta_{in} - \tan\beta_{ex}|}{(0.6 + 0.8 \cos\beta_{ex})} f\left(\frac{V_{in}}{V_{ex}}\right) \quad (56)$$

was investigated. The data for a correlation of this type are plotted in Figure 9.

Considering Figures 8 and 9 in detail, a number of points emerge. Firstly, both figures exhibit the increase of loss with velocity ratio

which might be expected (in contrast to a correlation using deflection). Secondly, there is some reduction in scatter when the correlation includes a correction to represent possible trailing edge blockage losses. Thirdly, the scatter shown by the points beyond a velocity ratio of 0.55 makes the selection of a final form of the loss correlation extremely difficult. In general, the data show not an unreasonable nor an entirely unexpected result. With a velocity ratio of 0.5 or less, it is possible to design blade sections with little or no additional loss due to local surface velocity diffusions. As the velocity ratio increases towards its impulse value, it becomes increasingly difficult to avoid an increase in loss due to suction surface diffusion effects. The actual level of loss will depend on the actual severity of the adverse static pressure gradient, which will in turn depend on the detailed design of the section. In poorly designed blades, additional losses may also result from increased diffusion on the initial portion of the pressure surface. Thus, not only is an increase in loss level to be expected as the velocity ratio increases, but some scatter might be expected in the data used for the correlation as a result of varying standards of blade design. A theoretical study of row losses presented in Reference 3 relates the total blade surface diffusion,  $D_T$ , to reaction (defined as  $1 - V_{in}/V_{ex}$ ) and tends to substantiate the increase in loss level for velocity ratio above 0.55. Figure 10 of Reference 3 shows a zero value of total diffusion at a velocity ratio of 0.45 and an almost linear increase as the velocity ratio is increased to unity.

The data used for the current loss correlation study is limited to a velocity ratio of 0.72. However, for a general application of the correlation, it will be necessary to extend the correlation beyond the range of the basic data. Since the characteristic form of the data will

make an extrapolation difficult, a data point corresponding to a blade section beyond impulse has been added to those initially derived. This point was obtained from stage performance data of a high-pressure-ratio turbine presented in Reference 2. The point, which has been included in Figures 8 and 9, is for a high deflection rotor operating beyond impulse. This data point tends to confirm a correlation of the type suggested in Equation 55 rather than Equation 56. However, the data points corresponding to velocity ratios of approximately 0.71 originate from an area of the stage efficiency correlation where there are a few test results. These loss coefficients were derived from points on a line ( $\chi = 2\phi - 1$ ) which passes through the efficiency contours of Figure 4 where they are most open to question.

While a precise correlation is difficult to select, the over-all form of the correlation can be chosen with a fair degree of confidence. A good correlation for the function of velocity ratio would appear to be two straight lines; below a velocity ratio of 0.5 the level of loss is almost independent of row reaction but beyond 0.5 the level of loss increases approximately linearly with velocity ratio. However, because the computer program will use a forward-stepping procedure involving the derivative of the loss coefficient, a correlation continuous in the first derivative of loss coefficient with respect to velocity ratio was selected. In addition, due to the lack of certainty in the selection of a correlation, the coefficients of the correlation will be input quantities for the computer program. The selected correlation is of the form

$$Y = \frac{|\tan \beta_{in} - \tan \beta_{ex}|}{(a_4 + a_5 \cos \beta_{ex})} \left\{ a_1 + a_2 \left( \frac{V_{in}}{V_{ex}} - a_3 \right) \right\} \quad \text{if } \frac{V_{in}}{V_{ex}} \geq a_3$$

$$\text{and } Y = \frac{|\tan \beta_{im} - \tan \beta_{ex}|}{(a_4 + a_5 \cos \beta_{ex})} \left\{ a_6 + a_7 \left( \frac{V_m}{V_{ex}} \right)^{a_8} \right\} \text{ if } \frac{V_m}{V_{ex}} < a_3 \quad (57)$$

where  $a_1$  to  $a_8$  are coefficients which may be selected by the program user.

The velocity-ratio-dependent function using  $a_1 = 0.055$ ,  $a_2 = 0.15$ ,  $a_3 = 0.6$ ,  $a_6 = 0.03$ ,  $a_7 = 0.157255$ , and  $a_8 = 3.6$  is shown in both Figure 8 and

9. This particular type of correlation is suitable for a design analysis.

If the coefficients  $a_1$ ,  $a_2$ ,  $a_3$ , and  $a_6$  are selected initially coefficients

$a_7$  and  $a_8$  can be readily evaluated from the conditions that the values of

$Y$  and  $dY/d\left(\frac{V_m}{V_{ex}}\right)$  are continuous at a value of  $\frac{V_m}{V_{ex}} = a_3$ .

Since the value of  $Y$  computed from Equation 57 can become extremely large as an exit angle approaches 90 degrees, the correlation will also include a maximum value of the total-pressure-loss coefficient.

#### Mean-Line Stage Performance Prediction Utilizing Loss Coefficient Correlation

Although the form of the loss coefficient correlation is theoretically acceptable, the values to be assigned to the constants are difficult to determine with any degree of certainty. In order to arrive at the final correlation to be recommended for the computer program, a number of stage performance predictions were undertaken. The principal objective of this investigation was to establish the values of the constants that gave the best over-all agreement with the achievable efficiency carpet plot. Predictions were undertaken initially at four levels of stage loading factor. The results of these efficiency predictions are shown in Figures 10, 11, 12, and 13 for values of  $g_p J C_p \Delta T_0 / u^2$  of 1.0, 1.5, 2.0, and 2.5, respectively. Each figure shows as a reference the experimental data correlation and predicted curves for three alternative forms of loss coefficient

correlation. The correlations compared are

$$Y = \frac{|\tan\beta_{in} - \tan\beta_{ex}|}{(0.6 + 0.8 \cos\beta_{ex})} \left\{ 0.03 + 0.1 \left| \frac{V_{in}}{V_{ex}} - 0.5 \right| + 0.1 \left( \frac{V_{in}}{V_{ex}} - 0.5 \right) \right\} \quad (58a)$$

$$Y = |\tan\beta_{in} - \tan\beta_{ex}| \left\{ 0.03 + 0.1 \left| \frac{V_{in}}{V_{ex}} - 0.5 \right| + 0.1 \left( \frac{V_{in}}{V_{ex}} - 0.5 \right) \right\} \quad (58b)$$

and 
$$Y = |\tan\beta_{in} - \tan\beta_{ex}| \left\{ 0.033 + 0.1 \left| \frac{V_{in}}{V_{ex}} - 0.55 \right| + 0.1 \left( \frac{V_{in}}{V_{ex}} - 0.55 \right) \right\} \quad (58c)$$

These alternative correlations assume, for convenience, two linear branches of the velocity ratio function rather than the more complex form of Equation 57. (In effect, coefficient  $a_7$  is set equal to zero and the condition for continuity in the derivative of  $Y$  with respect to  $V_{in}/V_{ex}$  is ignored.) Each of the alternative correlations has regions in which it fits the experimental data more closely than do the others. All produce a contour plot with the peak efficiency ridge following the 60 degree exit angle stator design line. It is in fact very difficult to decide at this time which of the three is the better correlation. Efficiency contour plots were prepared using correlations of Equations 58a and 58b, and these are shown in Figures 14 and 15. These two correlations differ only in the correction for trailing edge exit angle. In Figure 14 the trailing edge blockage correction is included, and it will be seen that, at any selected loading level, the efficiency falls more rapidly as the flow factor is decreased below its optimum value than when it is increased. In Figure 15, in which the correlation of Equation 58b is used, the contour plot becomes more symmetrical about the peak efficiency ridge. Unfortunately, if these figures are compared with the original data (see Fig 4), it would appear

that the correction should be applied for large exit angles but omitted for small angles. Some improvement could be obtained by changing the constants in the term  $a_4 + a_5 \cos \beta_{2x}$  but a review of data on which the correlation is based suggests that this is unwarranted at this time. Data points are shown in Figure 8 of Reference 1, and from this plot it can be appreciated that alternative positioning of the contours could be justified. An additional factor to be considered is that the turbines used in the correlation cover a considerable time span, and thus it is almost inevitable that design standards for both stage aerodynamics and blading have changed in this period of time.

In summary, a correlation of the form given in Equation 57 will be suitable for a design analysis program. However, since there is some uncertainty in what are the appropriate values of the coefficients, the coefficients  $a_1$  to  $a_7$  will be made part of the input specifications for the computer program. The recommended correlation is as follows:

$$Y = \frac{|\tan \beta_{in} - \tan \beta_{ex}|}{(0.6 + 0.8 \cos \beta_{2x})} \left\{ 0.055 + 0.15 \left( \frac{V_{in}}{V_{ex}} - 0.6 \right) \right\} \quad \text{if } \frac{V_{in}}{V_{ex}} \geq 0.6$$

$$\text{and } Y = \frac{|\tan \beta_{in} - \tan \beta_{ex}|}{(0.6 + 0.8 \cos \beta_{2x})} \left\{ 0.03 + 0.157235 \left( \frac{V_{in}}{V_{ex}} \right)^{3.6} \right\} \quad \text{if } \frac{V_{in}}{V_{ex}} < 0.6 \quad (59)$$

However, this particular correlation is based on a mean-line analysis of turbine stages which would have efficiencies consistent with the "achievable" efficiency correlation of Reference 1. Hence, it is quite possible that it will be necessary to modify the correlation at some future date. For example, the values assigned to coefficients  $a_1$ ,  $a_2$ , and  $a_3$  of Equation 57 may be found to be pessimistic for well-designed blades in which excessively high suction surface Mach numbers and large diffusion gradients

are avoided even at high values of velocity ratio  $v_m/v_{ex}$ .

#### Stream-Filament Prediction of Stage Performance

In arriving at the correlation, mean radius design analysis has been used with over-all stage efficiencies. However, the stage results are for blading which varies considerably with radius with respect to the correlating parameters. In addition, the correlation is to be used on an element basis in the design analysis. It is therefore necessary to investigate what effect the use of the correlation has on predicted stage efficiency when it is applied using the stream-filament approach. For this purpose two designs were selected and were analyzed using an existing NREC stream-filament design program. For the investigation total-pressure-loss coefficients were based on the correlation of Equation 58a. The designs were arbitrarily selected; one can be considered typical of the first turbine stage of a two-spool ducted fan engine and the other of the last stage which would be part of the fan turbine. Both designs assumed free-vortex flow, radially constant work, and 50 per cent stage reaction at mid-radius. Design I had a stage loading factor of 2.02, a flow factor of 0.75, and a pressure ratio of 1.9. A moderately high hub-to-tip diameter ratio was selected with which the rotor root reaction was limited to 15 per cent. The rotor exit angle was approximately constant at -62 degrees, the inlet angle varied from 10 to 55 degrees from casing to hub, and the rotor row relative velocity ratio varied from 0.4 to 0.75. The corresponding variation in rotor total-pressure-loss coefficient varied from 0.07 at the tip to 0.39 at the hub. The mass flow weighted stage efficiency was computed to be 0.915 which compares well with the stage data of Figure 4. It is about one half of one per cent less than that predicted on a mean-line



basis (see Fig 15).

For Design II, a loading factor of 1.4, a stage flow factor of 0.99, and a pressure ratio of 1.67 were selected. A lower hub-to-tip diameter ratio was also selected, and the resultant hub reaction was near impulse. The variation in rotor loss coefficient for the lower deflection blading varied from approximately 0.07 to 0.22. The mass flow weighted stage efficiency was found to be 0.898. This value is approximately 0.005 less than the value obtained from either Figure 4 or Figure 15.

Although it is unwise to base any firm conclusions on the results of a limited investigation, it would appear that the correlation can be applied to elements of a stage design despite the fact that it was derived from a mean section performance analysis.

#### Loss Factors

While the correlation is to be made an integral part of a design analysis computer program, it is desirable to provide the program user with the facility to adjust the level of loss by input factors or to specify row loss coefficients as inputs. The correlation was based on achievable efficiency data, and the efficiency levels were adjusted to zero tip leakage values. Thus, one of the principal corrections to be made for a turbine analysis will be for rotor tip clearance effects. The program will be supplied with the option to specify radial variations of the loss factor. These factors will be used to adjust the level of internally computed loss coefficients. Therefore, it will be possible to increase loss levels in the vicinity of rotor tips to represent the additional loss due to tip clearance. However, the amount of the correction to be made and the radial extent of the additional loss is difficult to assess at this time. Various

empirical methods for the correction of stage efficiency for tip clearance effects exist, but none of these are specifically applicable to a stream-filament analysis. One of the possible problems associated with the stream-filament approach is that, if severe gradients of loss are specified, there will be no solution of the input specification. More specifically, in order to satisfy both radial equilibrium and continuity equations a reverse flow, with negative values of meridional velocity, may be required. The manner in which radial distribution of additional losses and compensating distributions of work output are specified, in order to maintain a mechanically acceptable standard of blade row geometry, can only be fully investigated when the computer program is available.

Other factors which affect the level of loss are Reynolds number, blade row aspect ratio, and trailing edge thickness. As with tip clearance loss, various empirical correction methods exist for these factors. However, there are no generally accepted corrections; the reason for this is probably due to the fact that the detailed design of the blade is more important than the over-all interrow aerodynamics or the over-all geometry of the section against which these effects are often correlated. Similarly, the datum loss levels may be a function of the over-all design. For example, a constant section stator blade may have a distribution of loss which differs both in radial distribution and level from a conventional free-vortex stator. These differences may not be predictable on a simple stream-filament basis, since the complete distribution of the blade surface pressures within the blade passage may not be simply related to the blade row inlet and exit aerodynamics which are used as the basis for the loss correlation.

While the design-point analysis may be undertaken to investigate over-all performance using the internal correlation of total-pressure-loss

coefficient and the input loss factors, it is believed that the program will have to be used in conjunction with test data from stages designed using the stream-filament method before suitable correlations for the additional loss factor can be developed.

### Kinetic-Energy-Loss Coefficients

Although total-pressure-loss coefficients are used to express blade element performance in the analysis, there are, of course, other ways in which the row performance may be expressed. One of these alternatives is the kinetic-energy-loss coefficient,  $e$ , which is defined as follows:

$$e = 1 - \left( \frac{V_{ex}}{V_{ex,s}} \right)^2 \quad (60)$$

where the subscript  $s$  denotes the isentropic value of blade row exit velocity. The isentropic velocity is that velocity which would be attained in an isentropic expansion from the row inlet total pressure to the value of row exit static pressure. In Appendix I, it is shown that the total-pressure-loss coefficient,  $Y$ , and the kinetic-energy-loss coefficient,  $e$ , are related by the expression

$$Y = \frac{\left[ \frac{1}{(1-e)} - \frac{e}{(1-e)} \left\{ \frac{P_{ex}}{P_{ex,s}} \right\}^{\frac{\gamma-1}{\gamma}} \right]^{\frac{\gamma}{\gamma-1}} - 1}{\left( 1 - \frac{P_{ex}}{P_{ex,s}} \right)} \quad (61)$$

where  $P_{ex}/P_{ex,s}$  is the total-to-static pressure ratio at blade row exit. For rotor rows the relative total pressure is, of course, used in the pressure ratio.

Since the solution of the flow conditions at each of the design planes will involve the evaluation of the total-to-static pressure ratio across the annulus, it will be possible to readily accommodate kinetic-energy-loss coefficient as an optional design input.

## DEVELOPMENT OF THE ANALYSIS PROCEDURE

### Introduction

The solution of the flow field for the turbine design problem consists essentially of obtaining values of total pressure, total temperature, and the two components of the absolute velocity at each selected streamline location in each of the design planes. Thus, for the analysis  $P_o$ ,  $T_o$ ,  $V_u$ , and  $V_m$  are the principal variables. In the initial section of this report, all the equations which have to be satisfied in the analysis have been presented in terms of these variables. For an axisymmetric flow in an arbitrary annulus, the meridional slope and curvature of the stream-filament surfaces would have to be considered as analysis variables, but in the current analysis these quantities are regarded as known and will be derived from the flow boundaries as defined by the specified annulus contours or directly specified as inputs.

The solution of the flow field is obtained for the absolute values of  $P_c$ ,  $T_c$ ,  $V_u$ , and  $V_m$  at each of the design stations. Conditions relative to the rotors at inlet to and exit from each rotating blade row are obtained using conventional turbine design techniques after the design specifications and radial equilibrium have been satisfied in the absolute planes. Even though three types of design stations (namely, first stage stator inlet, stator exits, and stage exits) have to be considered, the design specifications for these stations differ, and various specification options are to be permitted for design-point analyses, the method of solution of the radial equilibrium and continuity equations has been developed so that the numerical procedures are identical for each design plane.

Before discussing the solution procedures, the specification of the inputs for a design-point analysis is reviewed. Following the presentation of the solution procedures, the outputs from the design-point analysis are also presented.

#### Specification of the Design Requirements and Analysis Variables

From the point of view of the numerical solution of the design problem, there is no real distinction between design requirements and analysis variables. Nevertheless, the following discussion subdivides the input into design requirements and analysis variables in the conventional manner.

#### Design Requirements

The type of unit, that is single or multispool, will be specified by a simple indicator of the number of spools to be considered. The analysis variables will be read in on a spool-by-spool basis, and hence the indicator will principally serve to distinguish between new spool data and new analysis variables for the original spool. With this approach the over-all program is considerably simplified, and the storage is relatively simply organized to accept up to eight stages on any spool and up to three spools in succession. It would have been possible to arrange to store data for more than one spool at any given time and thus permit successive analyses of alternative variables on multispool configurations. However, practical considerations indicate that it would be uneconomical to attempt a detailed analysis of alternative design variables for two or more spools. Preliminary analyses of a multispool configuration can be performed with any variations of the analysis variables

considered as complete new cases. When an over-all design outline has been obtained, detailed analysis could then be performed on each spool in turn. The over-all procedure need not necessarily be slowed down by the need to establish the outlet flow conditions of a preceding spool to define the inlet to any individual spool. The result of the preliminary multispool configuration can, of course, be used for more detailed investigation of the analysis variables of second or third spools.

The mass flow at machine inlet will be specified in lbm per sec and in the case of a cooled turbine will be supplemented by the specified cooling flow schedule. Coolant flows will be expressed as a fraction of the inlet mass flow and will be assumed to enter the main flow at the blade rows. Thus, if the coolant fractions for the first stator and first rotor are  $w_{c1}$  and  $w_{c2}$ , respectively, then the continuity equation will be satisfied for  $w_T$ ,  $w_T(1 + w_{c1})$ , and  $w_T(1 + w_{c1} + w_{c2})$  at design stations 0, 1, and 2, respectively. The temperature of the coolant at each point of admission will also be specified in general; an option will be provided so that these temperatures need not be specified if they are to be considered equal to those of the main stream.

Since the input will be accepted spool by spool, the rotative speed and required power output of each spool will be simply specified by the rpm and horsepower output of each shaft.

Inlet flow conditions of total pressure, total temperature, and flow angle will be specified against radius; the dimensions of these quantities will be lbf per sq in, deg R, degrees, and inches, respectively. In the computer program, parabolic interpolation of these quantities will be used. If only one value is specified, it will, of course, be assumed

constant; more complex distributions will require more data points to adequately describe them; if the inlet is that of a second or third spool, the distribution will be based on the output data from the preceding spool.

#### Analysis Variables

The number of stages will be simply specified. This number will be used to identify the subsequent data for it will be assumed that each stage consists of a stator followed by a rotor row.

The wall geometry will be specified by hub and casing radii at each design station. If these data are also to be used to compute wall slopes and curvatures, the axial spacing of these stations together with dummy stations ahead of the inlet and downstream of the final stage will also be specified. As an input option, streamline slopes and curvature in the meridional plane may be directly specified at selected radii. When slopes and curvatures are computed from specified annulus geometry, these quantities will be assumed to vary linearly between computed values at the annulus walls; when directly specified, streamline values of slope and curvature will be obtained by a linear interpolation or extrapolation of the specified data.

The power output distribution will be specified both by stage and across the annulus for the individual stages. The stage-by-stage distribution of output will be simply specified as a series of fractions of the total spool power. The distribution of power from hub to casing of individual stages will be specified using a nondimensional power function which varies from zero at the hub to unity at the casing. These power functions will be specified for each streamline except for the special

case of uniform distribution of power output. The reasons for the selection of this particular type of power distribution specification are discussed fully later.

Since the method of solution follows the streamline flow from the spool inlet, the basic specification of tangential velocities across the annulus will be made at stator rather than stage exits. The tangential velocities at selected radial positions will be specified at each stator exit plane. However, since mechanically acceptable blade geometries are more readily obtained when the stator exit absolute flow angles are specified, the specification of tangential velocities or flow angles will be one of the program options.

The row loss characteristics need not be specified if the internal correlation of total-pressure-loss coefficient is used. However, to provide the flexibility for particular design analyses, the datum level of loss coefficients may be adjusted using loss factors in the input specification. These loss factors can be radius and row dependent. The use of the internal total-pressure-loss correlation and loss factors is undoubtedly the most useful option for a design analysis, the basic purposes of which are to determine the design geometry and predicted performance. However, additional options are provided. These are to specify (as functions of radius) total-pressure-loss coefficients, kinetic-energy-loss coefficients, and rotor or stage isentropic efficiency. The specification of isentropic efficiencies to represent the rotor row performance characteristics, in conjunction with a stator total-pressure-loss coefficient, is an option which will not be frequently used for the analysis of new designs. However, the provision of this option will make the computer



program of greater value in that it could be used for the detailed investigation of experimental data from which further information on the stream-filament loss characteristics of turbines will have to be obtained.

Since the analysis will be performed with design station values of specific heat, a value of specific heat will have to be specified for each of the design stations.

The analysis variables reviewed above complete the input specification for the stream-filament analysis. However, when the effects of interfilament mixing are to be simulated in the analysis, the radius and row dependent mixing parameters will also have to be specified.

#### Basic Equations and Fundamental Solution Technique

In order to establish a procedure which is independent of the type of design station and selected input options, the analysis has been developed on the basis that the total pressure, the total temperature, the tangential velocity, and the meridional velocity are the unknowns, even though in certain circumstances one or more of these quantities will be directly specified. The basic equations which have to be satisfied are those concerned with

1. Power output
2. Radial equilibrium (radial momentum)
3. The element performance (total pressure loss)
4. Angular momentum - Euler work

and 5. Mass flow continuity

All the necessary equations, with the exception of the power output equation, have been presented in the initial section of the report in terms of the analysis variables  $P_o$ ,  $T_o$ ,  $V_u$ , and  $V_n$ . For the general design-point

analysis the variables  $P_o$ ,  $V_u$ , and  $V_{m1}$  are interdependent, but the fourth variable,  $T_o$ , is directly dependent on the specifications of the design variables. Thus, the evaluation of streamline values of total temperatures is regarded in the analysis as a preliminary to the solution of the problem proper and will be discussed prior to the method of solution for the three remaining variables.

#### Evaluation of Total Temperatures

The total temperature at the first design station, that is the first stator inlet plane, will be directly specified as a function of radius. A linear interpolation of these input data will be used to establish values of total temperature at the streamline positions used in the analysis. At the following station, a stator exit, the streamline values of total temperature will be unchanged from the corresponding streamline value at the preceding station for the purely streamline analysis, but will be modified in the manner previously discussed when interfilament mixing or the addition of coolant have been specified.

The total temperature distribution at the next station, a stage exit, will have to satisfy both the specified total power output and its distribution across the annulus. Since initially the distribution of mass flow throughout the annulus is unknown until the distribution of meridional velocity has been established, the power distribution will be specified by nondimensional power functions versus the nondimensional mass flow function,  $w(r)$ , which has been defined by Equation 21.

If the total power output specified is  $HP_T$  (horsepower), the total temperature drop  $\Delta T_o$  through the rotor must satisfy the equation,

$$HP_T = \frac{Jc_p}{550} \int_0^{w_T} \Delta T_o dw \quad (62)$$

Normalizing Equation 62 with respect to the total power and the total mass flow,  $w_T$ , leads to a definition of a power function  $\mathcal{P}(w(r))$  which is expressed as

$$\mathcal{P}(w(r)) = \frac{w_T \bar{J} C_p}{HP_T \cdot 550} \int_0^{w(r)} \Delta T_o dw(r) \quad (63)$$

where  $w(r)$  is the nondimensional mass flow function which varies from zero to unity between the hub and casing streamlines. Similarly, the power function will vary between zero and unity. Differentiating Equation 63 with respect to the nondimensional mass flow function yields a general expression for the total temperature drop; for the  $j^{\text{th}}$  streamline,

$$(\Delta T_o)_j = \frac{HP_T \cdot 550}{w_T \bar{J} C_p} \left\{ \frac{d \mathcal{P}(w(r))}{d w(r)} \right\}_j \quad (64)$$

where  $d \mathcal{P}(w(r)) / d w(r)$  is the local slope of the power function with respect to the nondimensional mass flow function. Thus, the power function versus mass flow function will be a basic specification for power distribution from which the total temperature drops are obtained. Hence, the actual temperature distribution at stage exit will be obtained on a streamline basis using the calculated temperature drop and the corresponding streamline total temperature at the preceding station. (Where mixing or the addition of coolant to the rotor row has been specified, the upstream values of total temperature will be modified as previously discussed.)

The principal advantage of the use of this type of specification for power distribution, which in effect relates total temperature drops to streamline positions rather than radial positions, is that the power output equation (Equation 62) is automatically satisfied. It is therefore possible to directly assign values of total temperatures to the streamlines without undertaking the iteration which would be necessary

if the specification involved power output as a direct function of radius. The type of specification is particularly well suited to a stream-filament analysis where the program user is concerned with the power output distribution between filaments rather than total temperature drop as a function of radius. This type of design will be characterized by the selected power function versus mass flow function relationship. If only 40 per cent of the total stage power output is required from the flow between the hub and mean streamline, one of the input data points will be 0.5, 0.4; the slope of the power function (and hence the total drop along the hub contour) will be lower at the hub (0.0, 0.0) than at the casing (1.0, 1.0). For a "constant work" distribution, the power function versus mass flow function will be linear between the points (0.0, 0.0) and (1.0, 1.0).

#### Evaluation of Total Pressures and Velocity Components

Except for the cases where the total pressure and tangential velocities are directly specified or can be simply obtained from the Euler work equation, the total pressure and the tangential and meridional components of velocity are interdependent. The distribution of  $P_o$ ,  $V_u$ , and  $V_m$  at each design station must be such that they satisfy the requirements of radial equilibrium and continuity. The relevant equations, expressed in terms of the analysis variables, are repeated below.

$$\frac{dV_m^2}{dr} + \frac{\gamma-1}{\gamma} \left\{ V_u^2 + V_m^2 - 2g_o \sqrt{c_p T_o} \right\} \frac{1}{P_o} \frac{dP_o}{dr} + 2V_u \frac{dV_u}{dr} = \frac{2V_m^2 \cos A}{r_m} - \frac{2V_u^2}{r} + (V_u^2 + V_m^2) \frac{1}{T_o} \frac{dT_o}{dr} \quad (65)$$

$$W_T = \frac{2\pi}{R} \int_{r_h}^{r_c} \frac{P_o}{T_o} \left[ 1 - \frac{V_u^2 + V_m^2}{2g_o \sqrt{c_p T_o}} \right]^{\frac{1}{\gamma-1}} V_m \cos A r dr \quad (66)$$

The tangential velocity, as a function of radius, will be directly or indirectly specified. At the first design station, which will be the first stage stator inlet of the design being analyzed, the tangential velocity will be indirectly specified by the flow angle. Hence, at any radius

$$V_{u0} = V_{m0} \cos A_0 \tan \beta_0 \quad (67)$$

At the stator exit plane, when the option of specifying flow angle is selected, the relationship between  $V_{u1}$  and  $V_{m1}$  is, of course, similar to that of Equation 67. That is,

$$V_{u1} = V_{m1} \cos A_1 \tan \beta_1 \quad (68)$$

When stator exit tangential velocities are directly specified, then tangential velocity can be considered as a known function of radius.

$$V_{u1} = V_{u1}(r) \quad (69)$$

Similarly, since streamline values of the total temperature drop across the rotor blade will be obtained from the specifications, the tangential velocity at stage exit can be also considered as a known function of radius if the radial locations of the streamlines are assumed. That is,

$$V_{u2} = \frac{u_1 V_{u1} - g_0 J c_p \Delta T_0}{u_2} = V_{u2}(r) \quad (70)$$

Considering the total pressure distributions, at the first design station the total pressure will be specified versus radius. Hence, the relevant equation is

$$P_{00} = P_{00}(r) \quad (71)$$

At stator exit the total pressure must be obtained from the loss coefficient

equation,

$$\gamma_N = \frac{P_{00} - P_{01}}{P_{01} - P_1} \quad (72)$$

Thus, the explicit expression for  $P_{01}$  in terms of the analysis variables becomes

$$P_{01} = \frac{P_{00}}{1 + \gamma_N \left[ 1 - \left( 1 - \frac{V_{m1}^2 + V_{u1}^2}{2g_0 J c_p T_{01}} \right)^{\frac{\gamma}{\gamma-1}} \right]} \quad (73)$$

When the performance of rotor elements is specified by a total-pressure-loss coefficient, the explicit equation for stage exit absolute total pressure,  $P_{02}$ , is derived from the loss coefficient definition which is repeated below

$$\gamma_R = \frac{P_{02s}' - P_{02}}{P_{02}' - P_2} \quad (74)$$

Hence,

$$P_{02} = P_{02}' \left[ \frac{P_{02}}{P_{02}'} \right] = \left\{ \frac{P_{02s}'}{1 + \gamma_R \left( 1 - \frac{P_2}{P_{02}'} \right)} \right\} \cdot \frac{P_{02}}{P_{02}'} \quad (75)$$

Using the previously presented relationship for  $P_{02}/P_{02}'$  (Equation 16), Equation 75 can be reexpressed in terms of the analysis variables as

$$P_{02} = \frac{P_{02s}' \left[ 1 + \frac{u_2 (u_2 - 2V_{u2})}{2g_0 J c_p T_{02}} \right]^{\frac{-\gamma}{\gamma-1}}}{1 + \gamma_R \left\{ 1 - \left( 1 - \frac{V_{m2}^2 + V_{u2}^2}{2g_0 J c_p T_{02}} \right)^{\frac{\gamma}{\gamma-1}} \left( 1 + \frac{u_2 (u_2 - 2V_{u2})}{2g_0 J c_p T_{02}} \right)^{\frac{-\gamma}{\gamma-1}} \right\}} \quad (76)$$

where the isentropic value of rotor relative exit total pressure,  $P_{02s}'$ , is given by Equation 15. The equations for stage exit total pressure are

considerably less complex when either of the alternative options of specifying stage isentropic or rotor isentropic efficiency is selected. These equations are obtained directly from Equations 12 and 13. That is,

$$P_{02} = P_{00} \left[ 1 - \frac{T_{01} - T_{02}}{\eta_S T_{00}} \right]^{\frac{\gamma}{\gamma-1}} \quad (77)$$

and

$$P_{02} = P_{01} \left[ 1 - \frac{T_{01} - T_{02}}{\eta_R T_{00}} \right]^{\frac{\gamma}{\gamma-1}} \quad (78)$$

Since total temperatures can be obtained directly from the design specifications, for these options the total pressures can be regarded as known functions of radius,  $P_{02} = P_{02}(r)$ , for the solution of the flow field.

From the equations above it will be seen that in order to evaluate total pressures or tangential velocities it is, in general, necessary to first determine the meridional velocity. Since the distribution of meridional velocity must satisfy both radial equilibrium and continuity equations and these also involve the total pressure and tangential velocity, the most obvious method of solution would be the solution of three simultaneous equations. However, the radial equilibrium equation is a differential equation involving the derivatives  $dV_m^2/dr$ ,  $dV_u/dr$ , and  $1/P_0 dP_0/dr$ . Hence, the two additional equations must be obtained from the differentiation with respect to radius of the tangential velocity and total pressure equations. Since the three equations can only be solved for the derivatives, the actual values of the variables must be obtained from the simultaneous solution of the continuity equation.

Before discussing the numerical techniques which are used for the solution, the following section presents the particular forms of the

differential equations which are used in the solution.

### The Differential Equations

In presenting the equations, it will be assumed that the design stations to be considered are the first stator inlet, the first stator exit, and the first stage exit. The following stations in a multistage machine can, of course, be considered as merely repeating the problems presented by the first stator exit and first stage exit planes.

The radial equilibrium equation (Equation 65) is of the form

$$C_{11} \frac{dV_m^2}{dr} + C_{12} \frac{1}{P_0} \frac{dP_0}{dr} + C_{13} \frac{dV_u}{dr} = C_{14} \quad (79)$$

where  $C_{11}$ ,  $C_{12}$ ,  $C_{13}$ , and  $C_{14}$  are coefficients which can be assigned values at each point in a particular design plane once a value of meridional velocity has been selected. The variables  $T_0$ ,  $\cos A$ ,  $r_m$  and  $r$ , and the constants  $\gamma$ ,  $C_p$ ,  $g_0$ , and  $J$  are assumed to be known quantities.

The differentiation of the appropriate equation for total pressure (which is either Equation 71, 73, 76, 77, or 78, depending on the station being considered and the selected option) leads to a differential equation also of the form

$$C_{21} \frac{dV_m^2}{dr} + C_{22} \frac{1}{P_0} \frac{dP_0}{dr} + C_{23} \frac{dV_u}{dr} = C_{24} \quad (80)$$

where the coefficients  $C_{21}$ ,  $C_{22}$ ,  $C_{23}$ , and  $C_{24}$  are again in terms of quantities which are readily obtained from the design specifications for an assumed value of the meridional velocity.

Similarly, differentiation of either of the alternative expressions for  $V_u$  (obtained from Equations 67, 68, 69, or 70) will produce differential equations of the form



$$C_{31} \frac{dV_m^2}{dr} + C_{32} \frac{1}{P_0} \frac{dP_0}{dr} + C_{33} \frac{dV_u}{dr} = C_{34} \quad (81)$$

The coefficient  $C_{32}$  is in each case zero.

Although the actual differentiations involved to determine the coefficients are not in themselves complex, the expressions for the coefficients are in some cases quite complex. For convenience of presentation, the actual coefficients are given in Appendix II.

### Technique for Solution

While the coefficients of the three differential equations will differ depending on the station being considered and the selected input option, once these coefficients have been evaluated a unique technique can be used for the solution. Essentially, the problem becomes one of obtaining a meridional velocity distribution which simultaneously satisfies the radial equilibrium and continuity equations. Selecting an initial value of meridional velocity at one streamline position, the local values of the coefficients of the set of equations can be obtained. These equations are then solved for the derivative  $\frac{dV_m^2}{dr}$ . Then, using standard forward difference techniques, the value of meridional velocity at an adjacent streamline is obtained using the originally selected meridional velocity and the derivative  $\frac{dV_m^2}{dr}$ . Using the new value of meridional velocity, consistent values of total pressure, tangential velocity, and the coefficients are obtained for this streamline using the appropriate equations previously presented. Thus, the derivative  $\frac{dV_m^2}{dr}$  can be obtained at this new streamline also. The over-all process is repeated until the meridional velocity, total pressure, and tangential velocity have been determined at each of the

streamlines used in the analysis. Using Equation 18, the continuity equation, the mass flow for the distribution is evaluated. Since the distributions will have been based on an assumed value of meridional velocity at one point in the flow field, the mass flow computed will in general differ from the specified value. Hence, the assumed value of meridional velocity will have to be modified iteratively until the starting value is consistent with the continuity requirement.

#### Over-All Solution Procedure

The over-all design analysis proceeds from known inlet conditions station by station through the turbine. The basic calculations are performed using grid points within the flow field which are defined by an even number of equal-flow stream filaments. Since initially the flow distribution is unknown, the initial streamline positions are estimated from equal areas for each filament. Hence, streamline positions have to be relocated after each solution of radial equilibrium and continuity until a converged solution for streamline positions has been obtained. Included in this major iterative loop will be an iteration on streamline values of total-pressure-loss coefficients when the optional specification of kinetic-energy-loss coefficients has been selected.

When the meridional velocity satisfies the radial equilibrium equation, the specified design variables, and the continuity equation within a preset tolerance, new streamline positions, and where applicable, loss coefficients are obtained. Revised values of the streamline dependent variables required for the coefficients of the three differential equation are then obtained. The solution of the radial equilibrium and continuity equations is then repeated until the streamline positions, and loss

coefficients if kinetic-energy-loss coefficients are specified, have converged to within preset tolerances.

Having obtained the basic solution at one design station, streamline values of all the relevant aerodynamic parameters in both relative and absolute reference systems are readily obtainable using conventional turbine design procedures. Among the quantities computed will be those necessary as input for the solution of the flow field at the following design station. These will include, where applicable, revised streamline values of total pressure and total temperature when the addition of coolant flow and/or interfilament mixing has been specified for the downstream blade row.

From the point of view of a numerical solution, the following design stations are solved in an identical manner. The only basic differences between stations and input options are in the evaluation of the streamline coefficients of the set of three differential equations and in the selection of the initial estimate of the meridional velocity.

Because it is possible to have two solutions to compressible flow problems, it is advisable to commence the simultaneous solution of the radial equilibrium and continuity equations at a streamline which is most representative of the flow in the annulus. Hence, a mean streamline is selected, which equally divides the flow in the annulus. In practice this selection complicates the logic of the computer program in that the solution of the meridional velocity distribution has to proceed to each of the two boundary streamlines in turn. Nevertheless, for stator exit planes in particular, the variation in absolute Mach number across the annulus will be sufficiently large that convergence of the required solution will be best achieved when the meridional velocity is reestimated

at the most representative streamline for the flow field.

When the flow angle is specified, for example at the first stator inlet or stator exit planes, both subsonic and supersonic solutions are possible. At stator inlet it will be assumed that only the subsonic solution is of interest, and the initial meridional velocity will be selected to correspond to a Mach number of 0.4. At stator exit planes, it will be necessary to specify which of the two solutions is required. If the subsonic is chosen, the initial estimate of meridional velocity will be based on a mean Mach number of 0.8; for supersonic solutions the starting point of the flow iteration will be a Mach number of 1.2.

When tangential velocities are specified at stator exit and when they are indirectly specified as is the case at stage exit planes, two solutions are again possible. However, only one is of real interest, since the second will correspond to a design in which the axial component of velocity is supersonic. For these cases the first estimate of meridional velocity will be based on a stator exit angle of 60 degrees or a rotor relative exit angle of -60 degrees. For all design analysis of practical interest, the numerical solution will converge to that for which the axial component of Mach number is subsonic even though the absolute Mach number may be either subsonic or supersonic.

### Results of the Analysis

Since on completion of the basic solution, streamline values of total pressure, total temperature, the velocity components, and the flow angles will have been obtained at all design stations, the computer program output can be arranged to have any of the turbine design parameters as output. In line with good practice, the output will, of course,

contain a print out of all the input specifications of design requirements and analysis variables. Velocity triangle data will be given at each streamline station by station. These data include:

- Radius of streamline
- Meridional, axial, and tangential velocity components
- Absolute velocity and flow angle
- Blade speed and relative flow angle.

The state of the gas at each of the streamline positions will be defined by:

- Absolute total pressure and total temperature
- Rotor relative total pressure and total temperature
- Absolute and relative Mach numbers
- Static pressures and static temperature.

Where interfilament mixing and/or the addition of coolant has been specified, values of absolute and relative total pressures and total temperatures which are assumed to exist at the inlet to the following row for the purpose of calculating the following design station flow field will also be tabulated.

Following each complete stage a performance summary for the individual streamlines will be presented. These data will comprise:

- Stator and rotor velocity ratios as indicators of the section reactions
- Stator and rotor total-pressure-loss coefficients
- Stator and rotor blade row efficiencies (defined as  $1 - \epsilon$ , where  $\epsilon$  is the kinetic-energy-loss coefficient)
- Rotor and stage isentropic efficiencies.

The stage output data will be completed by a tabulation of mean values of:

Stator and rotor blade row efficiencies  
Stage work output in Btu per lbm  
Stage total-to-total and total-to-static isentropic efficiency  
Stage blade-to-jet speed velocity ratio.

Except for the last item which will use the mean streamline values, the above items will be computed using mass flow weighted values of pressures and temperatures.

At the conclusion of the design analysis for a spool, mass flow averaged quantities will be presented for the multistage unit. These output data will include:

Spool work and power  
Over-all total-to-total and total-to-static pressure ratios  
Over-all total-to-total and total-to-static isentropic efficiencies.

An over-all blade-to-jet speed velocity ratio based on the over-all spool pressure ratio and a mean blade speed will also be presented.

For the purely stream-filament analysis, that is in the absence of specified mixing or a coolant flow schedule, all the output quantities will be obtained using standard turbine analysis formulas. When mixing or coolant flows are specified, the definitions of streamline work and efficiency and mass flow weighted mean values of efficiency will be as defined in the earlier section of the report concerned with the modification of the basic analysis procedures. Since complete data on all the total temperatures and total pressures will be available as output, alternatively defined stream-filament efficiencies which would be consistent with the total-pressure-loss coefficients used in the analysis in the case of specified mixing within blade rows will be readily

calculated from the output. In addition, mass flow weighted efficiencies for cooled turbines can be redefined and reevaluated if an alternative definition of efficiency is preferred.

## REFERENCES

1. Smith, S. F., "A Simple Correlation of Turbine Efficiency", J. Royal Aero. Soc., vol. 69, July, 1965.
2. Stabe, R. G., et al, Cold-Air Performance Evaluation of a Scale-Model Fuel Pump Turbine for the M-1 Hydrogen-Oxygen Rocket Engine (NASA TN D-3819), National Aeronautics and Space Administration, Washington, D. C., February, 1967.
3. Stewart, Warner L., et al, "A Study of Boundary-Layer Characteristics of Turbomachine Blade Rows and Their Relation to Over-All Blade Loss", Trans. ASME, The American Society of Mechanical Engineers, Series D, September, 1960, p. 588.



NOMENCLATURE

<u>Symbols</u>	<u>Description</u>	<u>Units</u>
A	Angle of streamline slope in the meridional plane	deg
$C_p$	Specific heat at constant pressure	Btu/lbm deg R
$D_T$	Total blade surface diffusion	--
e	Kinetic-energy-loss coefficient ( $= 1 - V_z^2/V_{z5}^2$ )	--
e''	Alternative kinetic-energy-loss coefficient for compressible flow ( $= 1 - (\rho_z V_z^2)/(\rho_{z5} V_{z5}^2)$ )	--
f	Arbitrary function	--
$g_o$	Constant in Newton's law	lbm/lbf ft/sec <sup>2</sup>
h	Enthalpy	Btu/lbm
$HP_T$	Total power in horsepower	hp
J	Mechanical equivalent of heat	ft lbf/Btu
j	Index on streamlines	--
n	Number of streamlines	--
$P_o$	Total pressure	psi
P	Static pressure	psi
p	Nondimensional power function $= \frac{W_T J C_p}{350 HP_T} \int_0^{w(r)} \Delta T_o dw(r)$	--
P	Stage power output	Btu/sec
$\bar{R}$	Stage reaction	--
R	Gas constant	ft lbf/lbm deg R
r	Radius	in or ft
S	Pitch	in or ft

<u>Symbols</u>	<u>Description</u>	<u>Units</u>
$T_0$	Total temperature	deg R
$t_{te}$	Trailing edge thickness	in or ft
$U$	Blade speed	ft/sec
$V$	Velocity	ft/sec
$W$	Work extraction along a streamtube	Btu/lbm
$w$	Mass flow rate	lbm/sec
$w_c$	Cooling flow fraction of total annulus flow	--
$w(r)$	Nondimensional mass flow function $= \frac{2\pi}{\omega r R} \int_{r_h}^r \frac{P_0}{T_0} \left[ 1 - \frac{V_u^2 + V_m^2}{2g_0 J c_p T_0} \right]^{\frac{1}{\gamma-1}} V_m \cos A r dr$	--
$\chi_j$	Mixing parameter	--
$Y$	Total-pressure-loss coefficient	--
$\beta$	Flow angle	deg
$\gamma$	Ratio of specific heats	--
$\delta$	Row deflection	deg
$\eta_R$	Rotor isentropic efficiency	--
$\eta_S$	Stage isentropic efficiency	--
$\rho$	Density	lbm/ft <sup>3</sup>
$\phi$	Stage flow function (= $V_x/U$ )	--
$\psi$	Stage loading function (= $g_0 J c_p \Delta T_0 / U^2$ )	--
$\Omega$	Rotational speed	rpm
<u>Subscripts</u>	<u>Description</u>	
$c$	Coolant	

<u>Subscripts</u>	<u>Description</u>
c	Casing
ex	Exit
h	Hub
in	Inlet
m	Meridional
N	Stator ("nozzle")
R	Rotor
r	Radial
s	Stage
S	Isentropic
T	Total
u	Tangential
x	Axial
0	Stage inlet
1	Stator exit/rotor inlet
2	Stage exit

<u>Superscripts</u>	<u>Description</u>
/	Relative to rotor
*	Subsequent to mixing
**	Subsequent to coolant addition
—	Mean or mass flow weighted value

## APPENDIX I

### THE RELATIONSHIP BETWEEN TOTAL-PRESSURE-LOSS COEFFICIENT AND KINETIC-ENERGY-LOSS COEFFICIENT

The losses in a blade row, or an element of a blade row, can be expressed in a number of ways. In the current analysis NREC has adopted a total-pressure-loss coefficient rather than a kinetic-energy-loss coefficient, which is preferred by some turbine designers. There are no significant difficulties associated with the introduction of both types of loss coefficient into the turbine design analysis program, since the two coefficients are simply related for a given value of blade row exit Mach number. In the following, the relationships are derived and a third coefficient, which is a true kinetic-energy coefficient for compressible fluids, is also briefly discussed.

The total-pressure-loss coefficient is defined as follows:

$$\gamma = \frac{P_{02S} - P_{02}}{P_{02} - P_2} \quad (1-1)$$

where  $P_{02S}$  is the isentropic value of total pressure at blade row exit,  $P_{02}$  is the actual total pressure, and  $P_2$  is the row exit static pressure. For stator rows the total pressures are absolute total pressures, and the isentropic total pressure at exit is equal to the row inlet total pressure  $P_{01}$  (i.e.,  $P_{02S} = P_{01}$ ). For rotor blades, the total pressures are relative values, and the isentropic total pressure at row exit will only equal the inlet total when there is no change of radius between inlet and exit. In general,

$$\frac{P_{02S}}{P_{01}} = \left[ 1 + \frac{u_2^2 - u_1^2}{2g_0 J c_p T_{01}} \right]^{\frac{\gamma}{\gamma-1}} \quad (1-2)$$

The definition of the kinetic-energy-loss coefficient is as follows:

$$e = 1 - \frac{V_z^2}{V_{zS}^2} \quad (1-3)$$

where  $V_z$  is the velocity at blade row exit and  $V_{zS}$  is the isentropic velocity at blade row exit, which is defined as the velocity which would be obtained for an isentropic expansion from the inlet total pressure to the actual static pressure at row exit. As with the total-pressure-loss coefficient, absolute quantities are used for a stator row and relative values for a rotor.

It should be noted that the coefficient defined by Equation 1-3 is not strictly a kinetic-energy coefficient for compressible fluids, since the actual density at row exit will not equal that obtained by an isentropic expansion to the same row exit static pressure. This point is discussed later.

The relationship between  $e$  and  $\gamma$  can be expressed in many forms, but since the total-pressure-loss coefficient involves total and static pressures, a logical choice for the relationship is in terms of total-to-static pressure ratio at row exit.

Equation 1-1 can be rewritten as follows:

$$\gamma = \frac{(P_{0zS}/P_{0z}) - 1}{1 - (P_z/P_{0z})} \quad (1-4)$$

Hence, the ratio of isentropic-to-actual total pressure at row exit is given by

$$\frac{P_{0zS}}{P_{0z}} = 1 + \gamma \left( 1 - \frac{P_z}{P_{0z}} \right) \quad (1-5)$$

Equation 1-3 can be expressed in terms of total-to-static pressure ratio as

$$e = 1 - \left[ \frac{1 - \left(\frac{P_2}{P_{02}}\right)^{\frac{\gamma-1}{\gamma}}}{1 - \left(\frac{P_2}{P_{02s}}\right)^{\frac{\gamma-1}{\gamma}}} \right] \quad (1-6)$$

Hence,

$$e = \frac{\left(\frac{P_2}{P_{02}}\right)^{\frac{\gamma-1}{\gamma}} - \left(\frac{P_2}{P_{02s}}\right)^{\frac{\gamma-1}{\gamma}}}{1 - \left(\frac{P_2}{P_{02s}}\right)^{\frac{\gamma-1}{\gamma}}} \quad (1-7)$$

Equation 1-7 can more conveniently be expressed as

$$e = \frac{\left(\frac{P_{02s}}{P_{02}}\right)^{\frac{\gamma-1}{\gamma}} - 1}{\left(\frac{P_{02s}}{P_{02}}\right)^{\frac{\gamma-1}{\gamma}} \left(\frac{P_{02}}{P_2}\right)^{\frac{\gamma-1}{\gamma}} - 1} \quad (1-8)$$

Substitution of the expression for total pressure ratio given in Equation 1-5 into Equation 1-8 produces the following expression for  $e$  in terms of  $\gamma$  and  $P_{02}/P_2$ .

$$e = \frac{\left[1 + \gamma\left(1 - \frac{P_2}{P_{02}}\right)\right]^{\frac{\gamma-1}{\gamma}} - 1}{\left[1 + \gamma\left(1 - \frac{P_2}{P_{02}}\right)\right]^{\frac{\gamma-1}{\gamma}} \left(\frac{P_{02}}{P_2}\right)^{\frac{\gamma-1}{\gamma}} - 1} \quad (1-9)$$

Equation 1-9 can, of course, be rearranged to obtain an explicit expression for  $\gamma$  in terms of  $e$  and  $P_{02}/P_2$ . That is,

$$\gamma = \frac{\left[\left(\frac{1}{1-e}\right) - \left(\frac{e}{1-e}\right)\left(\frac{P_{02}}{P_2}\right)^{\frac{\gamma-1}{\gamma}}\right]^{\frac{\gamma}{\gamma-1}} - 1}{1 - \frac{P_2}{P_{02}}} \quad (1-10)$$

The expressions given in Equations 1-9 and 1-10 can be written in terms of exit Mach number, critical velocity ratio, or total-to-static temperature using the standard thermodynamic formulas. Regardless of the particular form of the relationship, it will be seen that total-pressure-loss coefficients may be readily transformed to a kinetic-energy coefficient

and vice versa for any given value of total-to-static pressure ratio (or Mach number). With  $\mathcal{C}$  as an input to a design program, or contained in the program as a basic correlation, values of the total-pressure-loss coefficient used in the solution of the radial equilibrium equation (which forms the heart of the analysis procedure) can be obtained in an iterative procedure. This iterative procedure will essentially involve obtaining row exit total pressures from previously assumed or computed row exit flow conditions. It should be pointed out that this iteration is similar to that which is required when a correlation for total pressure loss is used in the analysis program.

It can be shown from Equations 1-9 and 1-10 that if  $\gamma$  is assumed independent of Mach number, then  $\mathcal{C}$  will decrease with increasing row exit Mach number, and conversely if  $\mathcal{C}$  is assumed independent of exit Mach number,  $\gamma$  will increase with Mach number. In practice, which of the two coefficients is more nearly constant with varying Mach number is not established. In the context of a turbine design-point analysis, it is implicitly assumed that any turbine design requirement will be suitably bladed, and hence the behavior of loss coefficients with Mach number determined from tests of given blade geometries is not strictly relevant. For example, a blade designed for low Mach number operation may exhibit increasing loss coefficients with increasing Mach number, whereas a section specifically designed for high Mach number operation may have the reverse loss coefficient versus Mach number characteristic.

In the earlier discussion of the kinetic-energy coefficient, it was stated that the expression given as Equation 1-3 assumes that the isentropic density,  $\rho_{2s}$ , is equal to the actual density,  $\rho_2$ . The actual

kinetic-energy-loss coefficient should therefore be written as follows for compressible flow:

$$e'' = 1 - \frac{\rho_z V_z^2}{\rho_{z5} V_{z5}^2} \quad (1-11)$$

Hence, assuming the exit static pressure and exit total temperature are equal for both isentropic and actual expansions, Equation 1-11 can be expressed as follows:

$$e'' = 1 - \frac{V_z^2}{V_{z5}^2} \left( \frac{P_{0z}}{P_{0z5}} \right)^{\frac{\gamma-1}{\gamma}} \quad (1-12)$$

Therefore, from Equations 1-3 and 1-12,

$$e'' = 1 - (1-e) \left( \frac{P_{0z}}{P_{0z5}} \right)^{\frac{\gamma-1}{\gamma}} \quad (1-13)$$

From Equations 1-7 and 1-13 the relationship between  $e$  and  $e''$  in its simplest form becomes

$$e'' = e \left( \frac{P_{0z}}{P_z} \right)^{\frac{\gamma-1}{\gamma}} = e \left( \frac{T_{0z}}{T_z} \right) \quad (1-14)$$

If it is assumed that  $e''$  is independent of exit Mach number,  $e$  will decrease with Mach number, while  $\gamma$  will increase with Mach number. This third coefficient is of interest therefore in that it does provide an intermediate between the differing schools of thought, the one considering total-pressure-loss coefficient independent of Mach number and the other which assumes  $e$  is independent of Mach number.



## APPENDIX II

### COEFFICIENTS FOR THE EVALUATION OF MERIDIONAL VELOCITY DISTRIBUTION AT ANY DESIGN PLANE

The meridional velocity distribution must satisfy the radial equilibrium equation (Equation 65). Since this equation involves derivatives of  $V_m^2$ ,  $\rho_c$ , and  $V_u$ , the method of solution selected is the simultaneous solution of three differential equations in which  $\frac{dV_m^2}{dr}$ ,  $\frac{1}{\rho_c} \frac{d\rho_c}{dr}$ , and  $\frac{dV_u}{dr}$  are the unknowns. The two additional equations are obtained from the differentiation of the appropriate equations for total pressure and tangential velocity. If a value of  $V_m$  is assumed at an initial streamline, the solution of the set of three equations will yield a value of the derivative  $\frac{dV_m^2}{dr}$ . Hence, using a forward-difference technique, the value of  $V_m$  at an adjacent point in the flow field may be evaluated and the solution repeated. Having obtained a complete solution for the annulus, the mass flow passing through the design station is computed. If the continuity equation (Equation 66) is not satisfied, the initial value of meridional velocity is reestimated and annulus flow conditions recomputed. Thus, the radial equilibrium and continuity equations are satisfied using an iterative procedure.

To simplify the logic of the computer program, a standard procedure is adopted for the solution of the flow field at each design station. The different types of design stations and the various optional specifications are taken into account by modifications to the twelve coefficients which appear in the three differential equations (Equations 79, 80, and 81). This appendix presents these coefficients. The three types of design stations are considered in turn; where there are optional specifications,

these alternative forms of the coefficients are given.

When the second differential equation is derived from the definition of the total-pressure-loss coefficient (at stator and stage exits), the expressions for the coefficients  $C_{21}$ ,  $C_{23}$ , and  $C_{24}$  contain additional coefficients  $C_{Y_1}$ ,  $C_{Y_3}$ , and  $C_{Y_4}$ . The values of these additional coefficients will depend on the selected correlation of total-pressure-loss coefficient. The actual expressions for  $C_{Y_1}$ ,  $C_{Y_3}$ , and  $C_{Y_4}$  for the selected loss correlation are presented in Appendix III.

### First Stator Inlet

The coefficients of Equation 79 are

$$C_{11} = 1.0$$

$$C_{12} = \left(\frac{\gamma-1}{\gamma}\right) \left\{ V_{u0}^2 + V_{m0}^2 - 2g_0 J(p_{T00}) \right\}$$

$$C_{13} = 2V_{u0}$$

$$C_{14} = \frac{2V_{m0}^2 \cos A_0}{r_m} - \frac{2V_{u0}^2}{r} + (V_{u0}^2 + V_{m0}^2) \frac{1}{r_{cc}} \frac{dr_{cc}}{dr}$$

The total pressure will be a specified function of radius. Hence, the coefficients of Equation 80 are

$$C_{21} = 0$$

$$C_{22} = 1.0$$

$$C_{23} = 0$$

$$C_{24} = \frac{1}{P_{cc}} \frac{dP_{cc}}{dr}$$

The tangential velocity will be indirectly specified by the specified variation of flow angle  $\beta_c$  with radius. Hence, from the differentiation of Equation 67, the coefficients of Equation 81 are

$$C_{31} = -\frac{\tan \beta_c \cos A_c}{2 V_{m0}}$$

$$C_{32} = 0.0$$

$$C_{33} = 1.0$$

$$C_{34} = V_{m0} \left\{ \frac{\cos A_c}{\cos^2 \beta_c} \frac{d\beta_c}{dt} - \tan \beta_c \sin A_c \frac{dA_c}{dt} \right\}$$

### Stator Exit

The coefficients of Equation 79 are

$$C_{11} = 1.0$$

$$C_{12} = \left( \frac{\gamma-1}{\gamma} \right) \left\{ V_{u1}^2 + V_{m1}^2 - 2g_c \sqrt{C_p T_{c1}} \right\}$$

$$C_{13} = 2V_{u1}$$

$$C_{14} = 2 \frac{V_{m1}^2 \cos A_1}{V_{m1}} - 2 \frac{V_{u1}^2}{\gamma} + (V_{u1}^2 + V_{m1}^2) \frac{1}{T_{c1}} \cdot \frac{dT_{c1}}{dt}$$

The coefficients of Equation 80 are obtained from the differentiation of Equation 73. In the analysis it is assumed that the derivative  $\frac{dY_N}{dt}$  can always be expressed as

$$\frac{dY_N}{dt} = C_{Y1} \frac{dV_{m1}^2}{dt} + C_{Y3} \frac{dV_{u1}}{dt} + C_{Y4}$$

Thus, the coefficients of Equation 80 are

$$C_{21} = \frac{\left( \frac{P_{c1}}{P_{c0}} \right) \left( \frac{T_1}{T_{c1}} \right)^{\frac{1}{\gamma-1}}}{2g_c R T_{c1}} Y_N + \left( \frac{P_{c1}}{P_{c0}} \right) \left( 1 - \frac{P_1}{P_{c1}} \right) C_{Y1}$$

$$C_{22} = 1.0$$

$$C_{23} = \frac{V_{u1} \left( \frac{P_{c1}}{P_{c0}} \right) \left( \frac{T_1}{T_{c1}} \right)^{\frac{1}{\gamma-1}}}{g_c R T_{c1}} Y_N + \left( \frac{P_{c1}}{P_{c0}} \right) \left( 1 - \frac{P_1}{P_{c1}} \right) C_{Y3}$$

$$C_{24} = \frac{1}{P_{c0}} \frac{dP_{c0}}{dt} + \frac{\left( \frac{P_{c1}}{P_{c0}} \right) \left( \frac{T_1}{T_{c1}} \right)^{\frac{1}{\gamma-1}}}{2g_c R T_{c1}} (V_{u1}^2 + V_{m1}^2) \frac{Y_N}{T_{c1}} \frac{dT_{c1}}{dt} - \left( \frac{P_{c1}}{P_{c0}} \right) \left( 1 - \frac{P_1}{P_{c1}} \right) C_{Y4}$$

If the tangential velocity is a specified function of radius, the coefficients of Equation 81 are

$$C_{31} = 0$$

$$C_{32} = 0$$

$$C_{33} = 1.0$$

$$C_{34} = \frac{dV_{u1}}{dr}$$

Alternatively, if the flow angle,  $\beta_1$ , is the specified quantity, the coefficients of Equation 81 are obtained from the differentiation of Equation 68. Thus, the coefficients are

$$C_{31} = -\frac{t \tan \beta_1 \cos A_1}{2 V_{m1}}$$

$$C_{32} = 0$$

$$C_{33} = 1.0$$

$$C_{34} = V_{m1} \left\{ \frac{\cos A_1}{\cos^2 \beta_1} \cdot \frac{d\beta_1}{dr} - t \tan \beta_1 \sin A_1 \frac{dA_1}{dr} \right\}$$

#### Stage Exit

The coefficients of Equation 79 are

$$C_{11} = 1.0$$

$$C_{12} = \left( \frac{\gamma}{\gamma-1} \right) \left\{ V_{u2}^2 + V_{m2}^2 - 2g_c J G_p T_{02} \right\}$$

$$C_{13} = 2V_{u2}$$

$$C_{14} = \frac{2V_{m2}^2 \cos A_2}{r_m} - \frac{2V_{u2}^2}{r} + (V_{u2}^2 + V_{m2}^2) \frac{1}{T_{02}} \cdot \frac{dT_{02}}{dr}$$

If either the option to specify rotor isentropic efficiencies or to specify stator isentropic efficiencies as a function of radius are used, the local total pressures can be calculated from Equation 77 or 78. Thus, the total pressure can be regarded as a known quantity and the coefficients of Equation 80 are

$$C_{21} = 0$$

$$C_{22} = 1.0$$

$$C_{23} = 0$$

$$C_{24} = \frac{1}{P_{02}} \cdot \frac{dP_{02}}{dr}$$

If the performance of the rotor is specified by a loss coefficient, the coefficients of Equation 80 are derived from the differentiation of an expression for  $P_{02}$ . Equation 76 can be reexpressed as

$$P_{02} = \frac{P_{01}' g_1}{g_2 g_4} \quad (11-1)$$

where

$$g_1 = \frac{P_{02S}'}{P_{01}'} = \left( \frac{T_{02}'}{T_{01}'} \right)^{\frac{\gamma}{\gamma-1}} = \left[ 1 + \frac{u_2^2 - u_1^2}{2g_c J C_p T_{01}'} \right]^{\frac{\gamma}{\gamma-1}}$$

$$g_2 = \frac{P_{02}'}{P_{02}} = \left( \frac{T_{02}'}{T_{02}} \right)^{\frac{\gamma}{\gamma-1}} = \left[ 1 + \frac{u_2^2 - 2u_2 V_{u2}}{2g_c J C_p T_{02}} \right]^{\frac{\gamma}{\gamma-1}}$$

$$g_3 = \frac{P_2}{P_{02}} = \left( \frac{T_2}{T_{02}} \right)^{\frac{\gamma}{\gamma-1}} = \left[ 1 - \frac{V_{u2}^2 + V_{m2}^2}{2g_c J C_p T_{02}} \right]^{\frac{\gamma}{\gamma-1}}$$

and

$$g_4 = \frac{P_{02S}'}{P_{02}'} = 1 + Y_R \left( 1 - \frac{P_2}{P_{02}'} \right) = 1 + Y_R \left( 1 - \frac{g_3}{g_2} \right)$$

Hence from Equation 11-1

$$\begin{aligned} \frac{1}{P_{02}} \cdot \frac{dP_{02}}{dr} &= \frac{1}{P_{01}'} \cdot \frac{dP_{01}'}{dr} + \frac{1}{g_1} \frac{dg_1}{dr} - \left( \frac{1}{g_2} + \frac{Y_R}{g_2 g_4} \right) \frac{dg_2}{dr} \\ &\quad + \frac{Y_R}{g_3 g_4} \frac{dg_3}{dr} - \frac{1}{g_4} \left( 1 - \frac{g_3}{g_4} \right) \frac{dY_R}{dr} \end{aligned}$$

Thus, when the differentials are evaluated

$$\begin{aligned}
\frac{1}{P_{02}} \cdot \frac{dP_{02}}{dr} &= \frac{1}{P_{01}} \cdot \frac{dP_{01}}{dr} + \frac{1}{2g_0 R T_{02}'} \left\{ 2u_2 \Omega - 2u_1 \Omega - (u_2^2 - u_1^2) \frac{1}{T_{01}'} \cdot \frac{dT_{01}'}{dr} \right\} \\
&- \left\{ 1 + \frac{P_{02}'}{P_{02s}'} Y_R \right\} \left[ \frac{2u_2 \Omega - 2u_2 \frac{dV_{u2}}{dr} - 2V_{u2} \Omega - (u_2^2 - 2u_2 V_{u2}) \frac{1}{T_{02}'} \cdot \frac{dT_{02}'}{dr}}{2g_0 R T_{02}'} \right] \\
&- \frac{Y_R \left( \frac{P_{02}'}{P_{02s}'} \right)}{2g_0 R T_2} \left[ \frac{dV_{m2}^2}{dr} + 2V_{u2} \frac{dV_{u2}}{dr} - (V_{m2}^2 + V_{u2}^2) \frac{1}{T_{02}'} \cdot \frac{dT_{02}'}{dr} \right] \\
&- \left( \frac{P_{02}'}{P_{02s}'} \right) \left( 1 - \frac{P_2}{P_{02}'} \right) \left[ C_{Y1} \frac{dV_{m2}^2}{dr} + C_{Y3} \frac{dV_{u2}}{dr} + C_{Y4} \right]
\end{aligned}$$

where it is assumed that the derivative  $\frac{dY_R}{dr}$  can be expressed as follows:

$$\frac{dY_R}{dr} = C_{Y1} \frac{dV_{m2}^2}{dr} + C_{Y3} \frac{dV_{u2}}{dr} + C_{Y4}$$

Thus the coefficients of Equation 80 will be

$$C_{21} = \frac{\left( \frac{P_{02}'}{P_{02s}'} \right) Y_R}{2g_0 R T_2} + \left( \frac{P_{02}'}{P_{02s}'} \right) \left( 1 - \frac{P_2}{P_{02}'} \right) C_{Y1}$$

$$C_{22} = 1.0$$

$$C_{23} = \frac{V_{u2} \left( \frac{P_{02}'}{P_{02s}'} \right) Y_R}{g_0 R T_2} - \frac{u_2 \left\{ 1 - \left( \frac{P_{02}'}{P_{02s}'} \right) Y_R \right\}}{g_0 R T_{02}'} + \left( \frac{P_{02}'}{P_{02s}'} \right) \left( 1 - \frac{P_2}{P_{02}'} \right) C_{Y3}$$

$$\begin{aligned}
C_{24} &= \frac{1}{P_{01}} \cdot \frac{dP_{01}}{dr} + \frac{1}{2g_0 R T_{02}'} \left\{ 2u_2 \Omega - 2u_1 \Omega - (u_2^2 - u_1^2) \frac{1}{T_{01}'} \cdot \frac{dT_{01}'}{dr} \right\} \\
&- \left\{ 1 + \frac{P_{02}'}{P_{02s}'} Y_R \right\} \left\{ \frac{2u_2 \Omega - 2V_{u2} \Omega - (u_2^2 - 2u_2 V_{u2}) \frac{1}{T_{02}'} \cdot \frac{dT_{02}'}{dr}}{2g_0 R T_{02}'} \right\} \\
&+ \frac{Y_R \left( \frac{P_{02}'}{P_{02s}'} \right)}{2g_0 R T_2} (V_{m2}^2 + V_{u2}^2) \frac{1}{T_{02}'} \cdot \frac{dT_{02}'}{dr} - \left( \frac{P_{02}'}{P_{02s}'} \right) \left( 1 - \frac{P_2}{P_{02}'} \right) C_{Y4}
\end{aligned}$$

Since the streamline total temperature can be readily calculated from power output function, the radial variation of tangential velocity, can be calculated from Equation 70. Thus,  $V_{u2}$  is in effect a known function of radius and hence the coefficients of Equation 81 are

$$C_{31} = 0$$

$$C_{32} = 0$$

$$C_{33} = 1.0$$

$$C_{34} = \frac{dV_{u2}}{dr}$$

APPENDIX III

THE COEFFICIENTS OF THE  
TOTAL-PRESSURE-LOSS COEFFICIENT DERIVATIVE

The second differential equation used in the simultaneous solution of  $\frac{dV_m^2}{dr}$  is obtained from an expression for the local value of total pressure. When the design station is a stator or stage exit and the loss of total pressure through the preceding blade row is computed from a total-pressure-loss coefficient, this second equation will involve the derivative  $\frac{dY_w}{dr}$  or  $\frac{dY_r}{dr}$ . In Appendix II it has been assumed that these can be expressed as follows:

$$\frac{dY}{dr} = C_{Y1} \frac{dV_m^2}{dr} + C_{Y3} \frac{dV_u}{dr} + C_{Y4} \quad (III-1)$$

where the coefficients  $C_{Y1}$ ,  $C_{Y3}$ , and  $C_{Y4}$  will appear in the expressions for  $C_{21}$ ,  $C_{23}$ , and  $C_{24}$ .

If the total-pressure-loss coefficient is a specified function of radius, or the over-all solution is an iterative one in the case of the specified kinetic-energy-loss coefficient option, these coefficients are as follows:

$$C_{Y1} = C_{Y3} = 0 \quad \text{and} \quad C_{Y4} = \frac{dY(r)}{dr}$$

When the local value of the total-pressure-loss coefficient is at its maximum allowable value of  $a_q$ , then

$$C_{Y1} = C_{Y3} = C_{Y4} = 0 \quad \text{when} \quad Y = a_q$$

When the total-pressure-loss coefficient is obtained from an internal correlation, the expressions for  $C_{Y1}$ ,  $C_{Y3}$ , and  $C_{Y4}$  will depend on the



particular correlation being used. For the computer program the loss coefficient will be expressed as follows:

$$Y = \frac{f_1 f_2 f_3}{f_4} \quad (111-2)$$

Hence,

$$\frac{dY}{dr} = Y \left\{ \frac{1}{f_1} \frac{df_1}{dr} + \frac{1}{f_2} \frac{df_2}{dr} + \frac{1}{f_3} \frac{df_3}{dr} - \frac{1}{f_4} \frac{df_4}{dr} \right\} \quad (111-3)$$

The values of  $C_{Y1}$ ,  $C_{Y3}$ , and  $C_{Y4}$  are then obtained by equating the right-hand sides of Equations 111-1 and 111-3.

### Stator Exit

The loss coefficient is defined by

$$a_9 \geq Y_N = \frac{f_1 (-\tan \beta_0 + \tan \beta_1) [a_1 + a_2 \left( \frac{V_0}{V_1} - a_3 \right)]}{(a_4 + a_5 \cos \beta_1)} \quad \text{when } \frac{V_0}{V_1} \geq a_3 \quad (111-4a)$$

$$Y_N = \frac{f_1 (-\tan \beta_0 + \tan \beta_1) [a_6 + a_7 \left( \frac{V_0}{V_1} \right)^{a_8}]}{(a_4 + a_5 \cos \beta_1)} \quad \text{when } \frac{V_0}{V_1} < a_3 \quad (111-4b)$$

where  $f_1$  is the additional loss factor which can be specified as a function of radius. The form of the individual derivatives will depend on whether the flow angle  $\beta_1$  or the whirl velocity  $V_{u1}$  is the specified quantity and the value of  $\frac{V_0}{V_1}$ .

Flow Angle Specified and  $\frac{V_0}{V_1} \geq a_3$

$$C_Y = - \frac{Y_N a_2 V_0}{2 f_3 V_1^3}$$

$$C_{Y3} = \frac{-Y_N a_2 V_{u1} V_0}{f_3 V_1^3}$$

$$C_{Y4} = Y_N \left\{ \frac{1}{f_1} \frac{df_1}{dr} + \frac{1}{f_2} \left( \sec^2 \beta_1 \frac{d\beta_1}{dr} - \sec^2 \beta_0 \frac{d\beta_0}{dr} \right) + \frac{1}{f_3} \frac{a_2}{V_1} \frac{dV_0}{dr} + \frac{a_5 \sin \beta_1}{f_4} \frac{d\beta_1}{dr} \right\}$$

Flow Angle Specified and  $\frac{V_0}{V_1} < a_3$

$$C_{Y1} = - \frac{Y_N a_7 a_8 \left( \frac{V_0}{V_1} \right)^{a_8}}{2 f_3 V_1^2}$$

$$C_{Y3} = - \frac{Y_N V_{u1} a_7 a_8 \left( \frac{V_0}{V_1} \right)^{a_8}}{f_3 V_1^2}$$

$$C_{Y4} = Y_N \left\{ \frac{1}{f_1} \frac{df_1}{dr} + \frac{1}{f_2} \left( \sec^2 \beta_1 \frac{d\beta_1}{dr} - \sec^2 \beta_0 \frac{d\beta_0}{dr} \right) + \frac{1}{f_3} \frac{a_7 a_8 \left( \frac{V_0}{V_1} \right)^{a_8-1}}{V_1} \frac{dV_0}{dr} + \frac{a_5 \sin \beta_1}{f_4} \frac{d\beta_1}{dr} \right\}$$

Whirl Velocity Specified and  $\frac{V_0}{V_1} \geq a_3$

$$C_{Y1} = -Y_N \left[ \frac{\tan \beta_1}{2 f_2 V_{u1}^2} + \frac{a_2 V_0}{2 f_3 V_1^3} + \frac{a_5 \sin^2 \beta_1 \cos \beta_1}{2 f_4 V_{u1}^2} \right]$$

$$C_{Y3} = Y_N \left[ \frac{\tan \beta_1}{f_2 V_{u1}} - \frac{a_2 V_{u1} V_0}{f_3 V_1^3} + \frac{a_5 \sin^2 \beta_1 \cos \beta_1}{f_4 V_{u1}} \right]$$

$$C_{Y4} = Y_N \left[ \frac{1}{f_1} \frac{df_1}{dr} + \frac{1}{f_2} \left( \tan \beta_1 \tan A_1 \frac{dA_1}{dr} - \sec^2 \beta_0 \frac{d\beta_0}{dr} \right) + \frac{1}{f_3} \frac{a_2}{V_1} \frac{dV_0}{dr} + \frac{a_5 \sin^2 \beta_1 \cos \beta_1 \tan A_1}{f_4} \frac{dA_1}{dr} \right]$$

Whirl Velocity Specified and  $\frac{V_0}{V_1} < a_3$

$$C_Y = -Y_N \left[ \frac{\tan A_1}{2 f_2 V_{u1}^2} + \frac{a_7 a_8 \left( \frac{V_0}{V_1} \right)^{a_8}}{2 f_3 V_1^2} + \frac{a_5 \sin^2 \beta_1 \cos \beta_1}{2 f_4 V_{u1}^2} \right]$$

$$C_{Y3} = Y_N \left[ \frac{\tan \beta_1}{f_2 V_{u1}} - \frac{a_7 a_8 V_{u1} \left(\frac{V_1}{V_1'}\right)^{a_8}}{f_3 V_1'^2} + \frac{a_5 \sin^2 \beta_1 \cos \beta_1}{f_4 V_{u1}} \right]$$

$$C_{Y4} = Y_N \left[ \frac{1}{f_1} \frac{df_1}{dr} + \frac{1}{f_2} \left( \tan \beta_1 \tan A_1 \frac{dA_1}{dr} - \sec^2 \beta_2 \frac{d\beta_2}{dr} \right) + \frac{a_7 a_8 \left(\frac{V_1}{V_1'}\right)^{a_8-1}}{f_3 V_1'} \frac{dV_1}{dr} + \frac{a_5 \sin^2 \beta_1 \cos \beta_1 \tan A_1}{f_4} \frac{dA_1}{dr} \right]$$

### Stage Exit

The definition of rotor loss coefficients is essentially identical with that used for the stators (Equation III-4a and III-4b); relative quantities and the relevant design station indices must, of course, be substituted throughout. Note that  $\beta_2'$  is by definition, a negative number

$$a_9 \geq Y_R = \frac{f_1 (\tan \beta_1' - \tan \beta_2') [a_1 + a_2 \left(\frac{V_1'}{V_2'} - a_3\right)]}{(a_4 + a_5 \cos \beta_2')} \quad \text{if } \frac{V_1'}{V_2'} \geq a_3 \quad (\text{III-5a})$$

$$Y_R = \frac{f_1 (\tan \beta_1' - \tan \beta_2') [a_6 + a_7 \left(\frac{V_1'}{V_2'}\right)^{a_8}]}{(a_4 + a_5 \cos \beta_2')} \quad \text{if } \frac{V_1'}{V_2'} < a_3 \quad (\text{III-5b})$$

$$\text{if } \left(\frac{V_1'}{V_2'}\right) \geq a_3$$

$$C_{Y1} = Y_R \left[ \frac{\tan \beta_2'}{2f_2 V_{m2}^2} - \frac{a_2 V_1'}{2f_3 V_2'^3} - \frac{a_5 \sin^2 \beta_2' \cos \beta_2'}{2f_4 V_{m2}^2} \right]$$

$$C_{Y3} = -Y_R \left[ \frac{\tan \beta_2'}{f_2 (V_{u2} - u_2)} + \frac{a_2 (V_{u2} - u_2) V_1'}{f_3 V_2'^3} - \frac{a_5 \sin^2 \beta_2' \cos \beta_2'}{f_4 (V_{u2} - u_2)} \right]$$

$$C_{Y4} = Y_R \left[ \frac{1}{f_1} \frac{df_1}{dr} + \frac{1}{f_2} \left\{ \sec^2 \beta_1' \frac{d\beta_1'}{dr} - \tan \beta_2' \left( \tan A_2 \frac{dA_2}{dr} - \frac{\Omega}{(V_{u2} - u_2)} \right) \right\} \right. \\ \left. + \frac{1}{f_3} \left\{ \frac{a_2}{V_2'} \frac{dV_1'}{dr} + \frac{a_2 V_1'}{V_2'^3} \Omega (V_{u2} - u_2) \right\} \right. \\ \left. + \frac{1}{f_4} a_5 \sin^2 \beta_2' \cos \beta_2' \left( \tan A_2 \frac{dA_2}{dr} - \frac{\Omega}{(V_{u2} - u_2)} \right) \right]$$

And If  $\frac{V_1'}{V_2'} < a_3$

$$C_{Y1} = Y_R \left[ \frac{\tan \beta_2'}{2f_2 V_{m2}^2} - \frac{a_7 a_8 \left(\frac{V_1'}{V_2'}\right)^{a_8}}{2f_3 V_2'^2} - \frac{a_5 \sin^2 \beta_2' \cos \beta_2'}{2f_4 V_{m2}^2} \right]$$

$$C_{Y3} = -Y_R \left[ \frac{\tan \beta_2'}{f_2 (V_{u2} - u_2)} + \frac{a_7 a_8 (V_{u2} - u_2) \left(\frac{V_1'}{V_2'}\right)^{a_8}}{f_3 V_2'^2} - \frac{a_5 \sin^2 \beta_2' \cos \beta_2'}{f_4 (V_{u2} - u_2)} \right]$$

$$C_{Y4} = Y_R \left[ \frac{1}{f_1} \frac{df_1}{dr} + \frac{1}{f_2} \left\{ \sec^2 \beta_1' \frac{d\beta_1'}{dr} - \tan \beta_2' \left( \tan A_2 \frac{dA_2}{dr} - \frac{\Omega}{(V_{u2} - u_2)} \right) \right\} \right. \\ \left. + \frac{1}{f_3} \left\{ \frac{a_7 a_8 \left(\frac{V_1'}{V_2'}\right)^{a_8-1}}{V_2'} \frac{dV_1'}{dr} + \frac{a_7 a_8 \Omega (V_{u2} - u_2) \left(\frac{V_1'}{V_2'}\right)^{a_8}}{V_2'^2} \right\} \right. \\ \left. + \frac{1}{f_4} a_5 \sin^2 \beta_2' \cos \beta_2' \left( \tan A_2 \frac{dA_2}{dr} - \frac{\Omega}{(V_{u2} - u_2)} \right) \right]$$

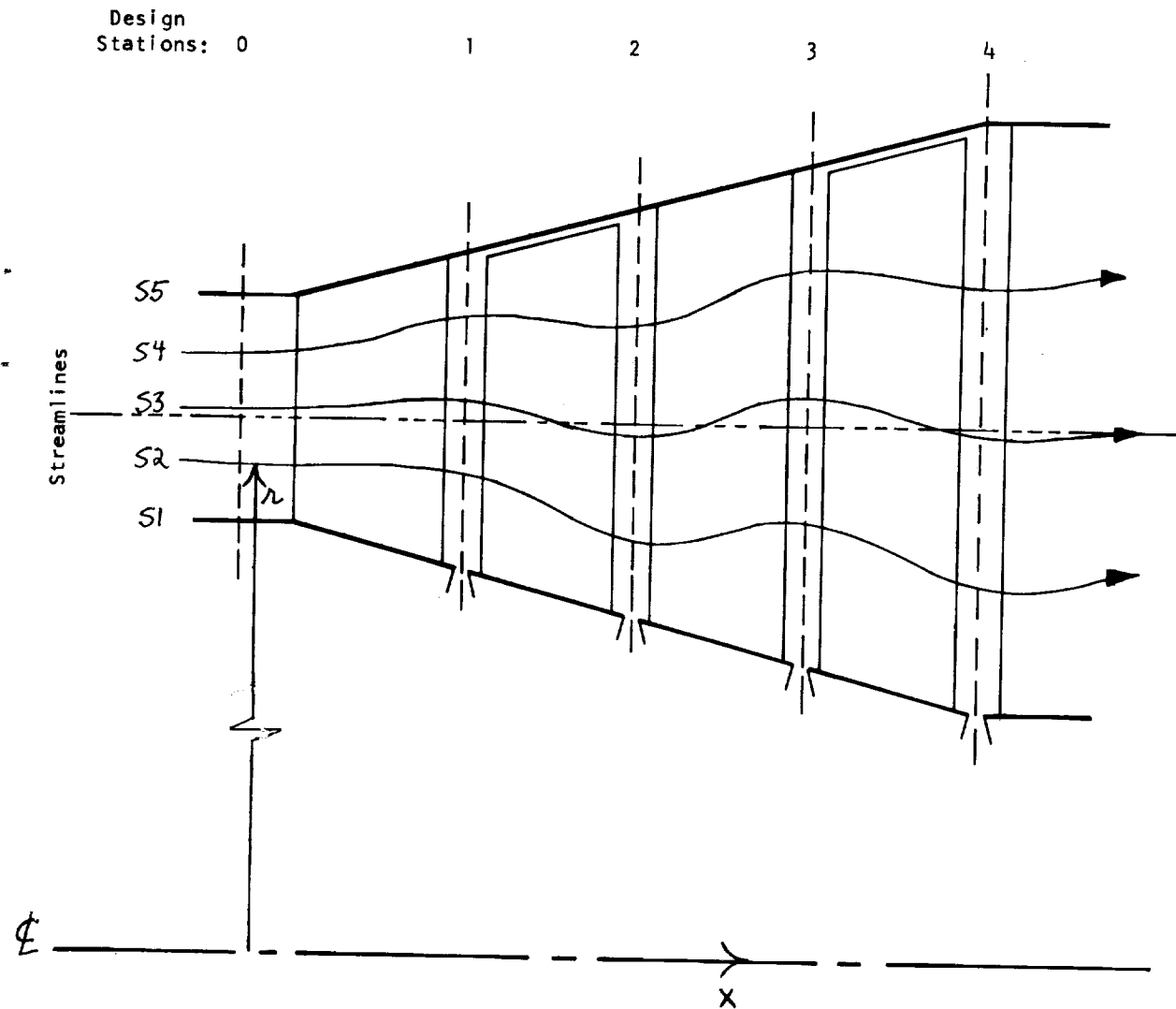


FIGURE 1 - MERIDIONAL SECTION OF A TWO-STAGE TURBINE  
TO DIAGRAMMATICALLY ILLUSTRATE AXISYMMETRIC STREAMLINE FLOW

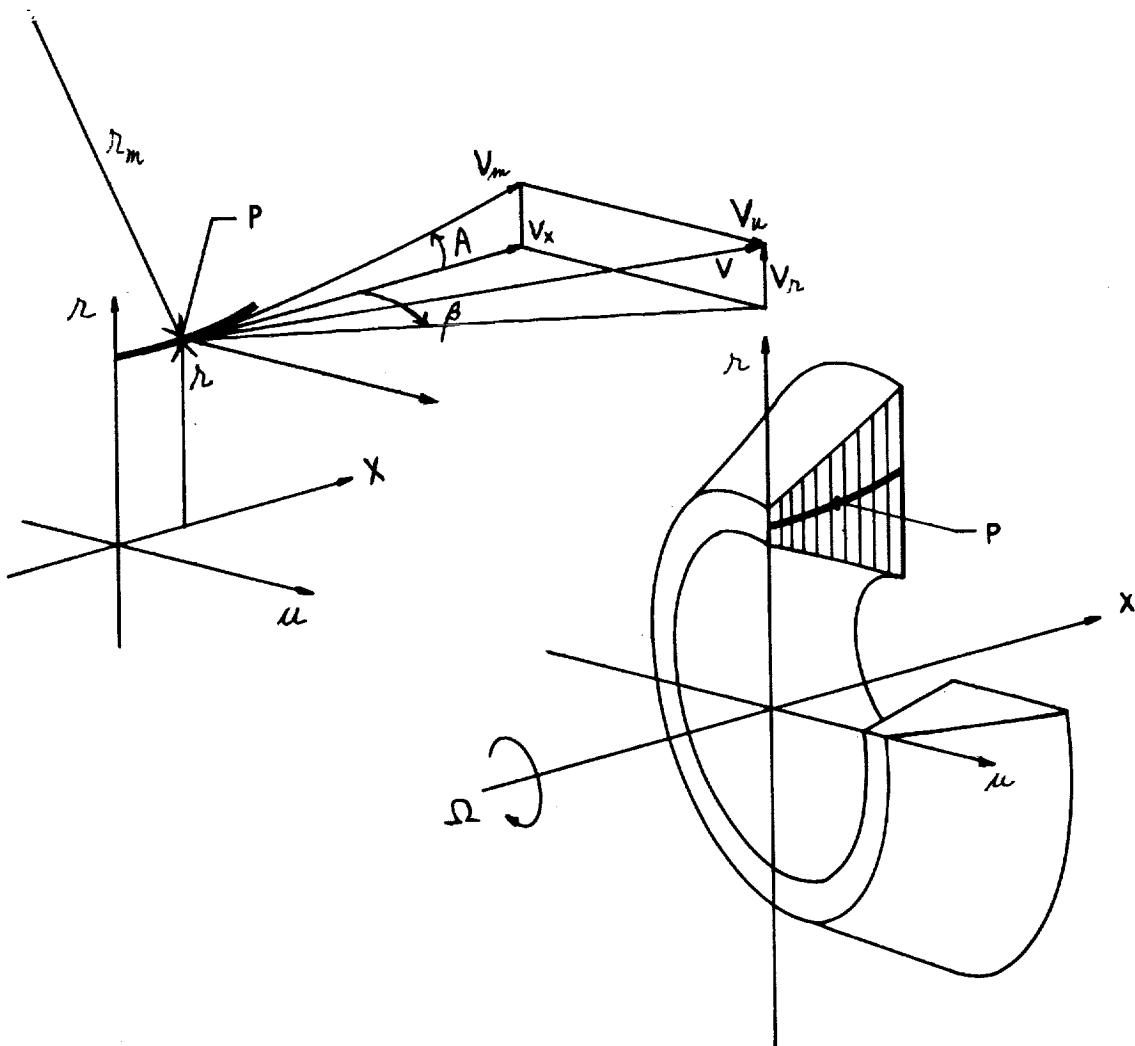
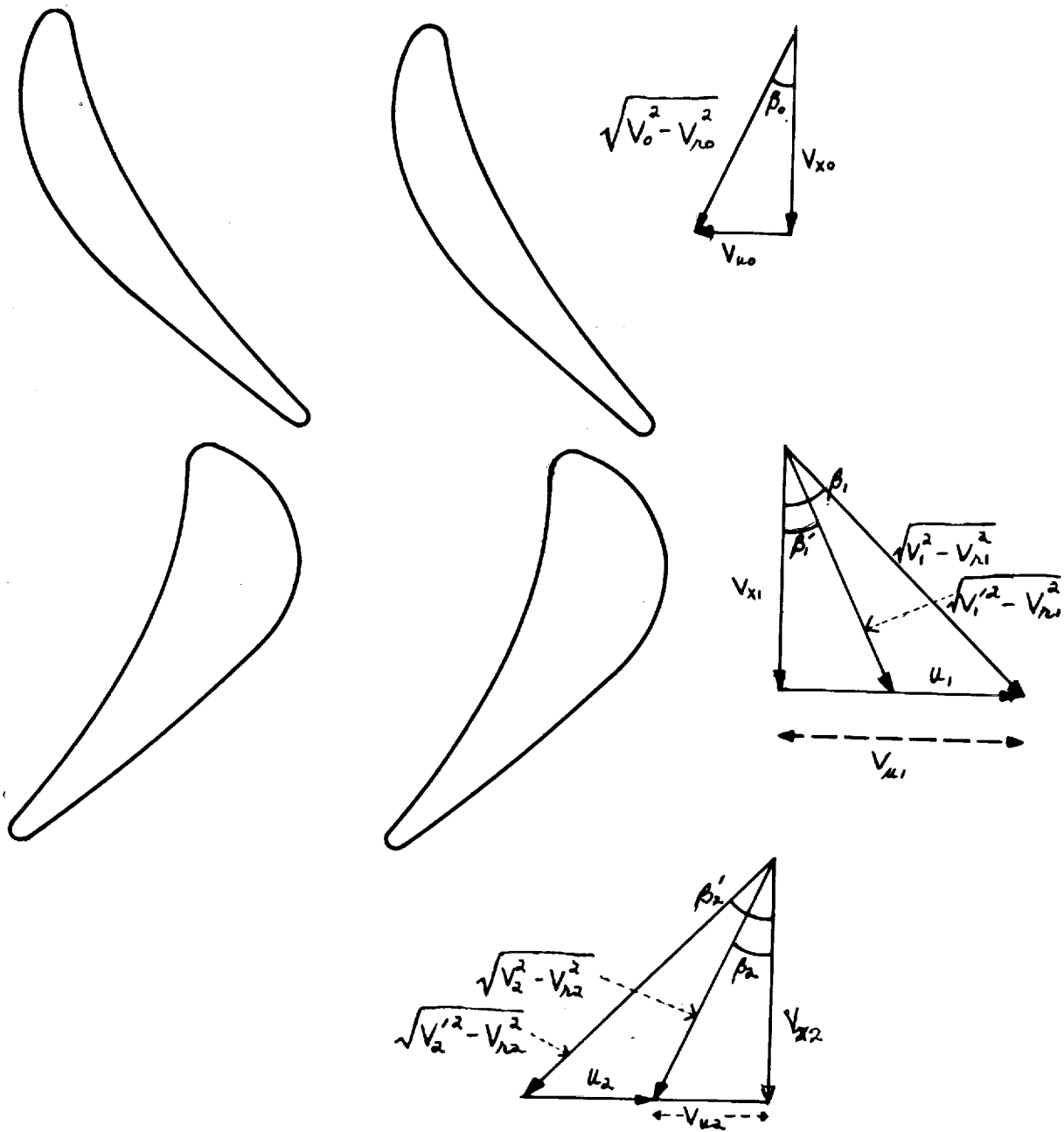
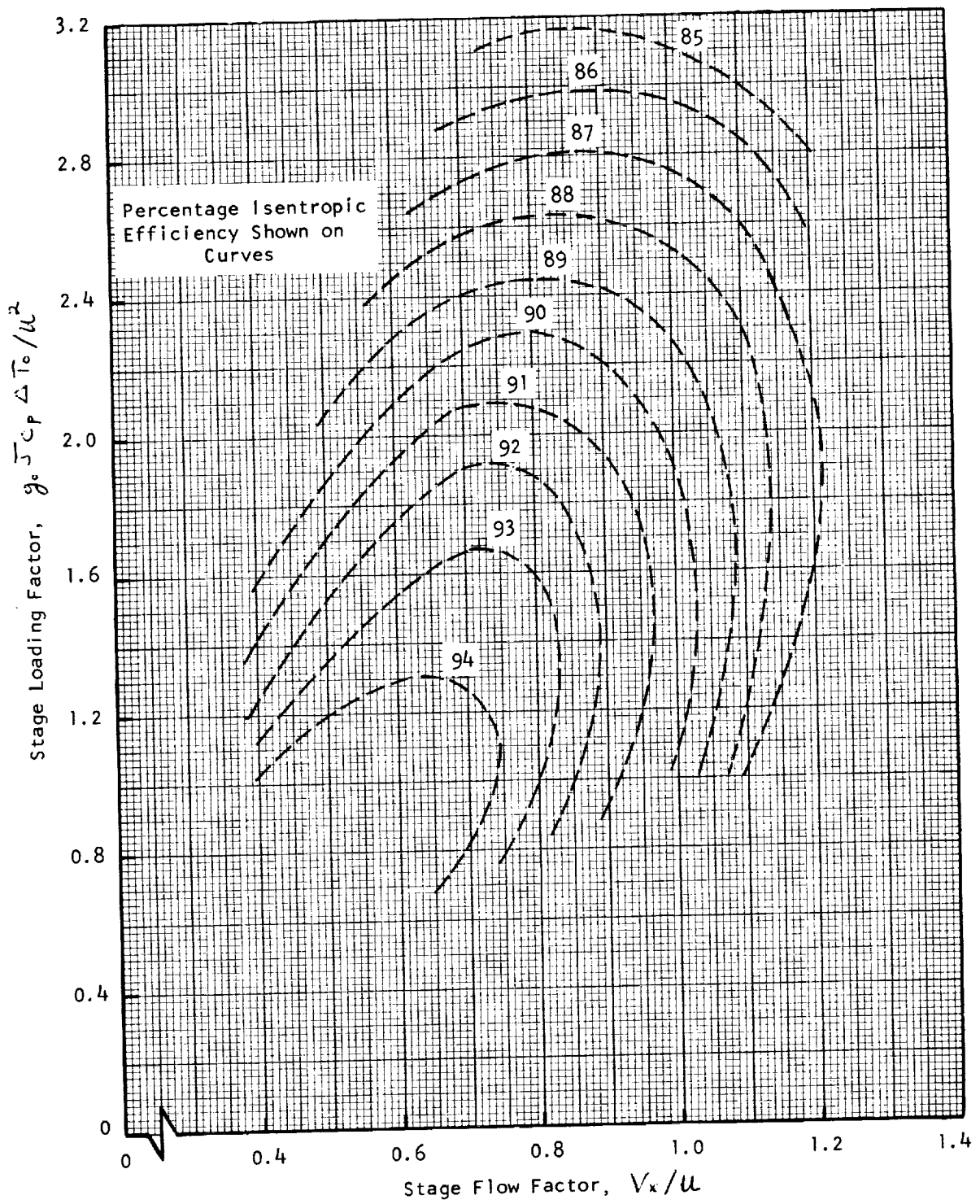


FIGURE 2 - NOMENCLATURE FOR AXISYMMETRIC FLOW IN AN ARBITRARY TURBINE ANNULUS



**FIGURE 3 - TURBINE VELOCITY TRIANGLE  
NOMENCLATURE USED IN THE STREAM-FILAMENT ANALYSIS**



Note: Reproduced from Reference 1

FIGURE 4 - A SIMPLE CORRELATION OF ACHIEVABLE TURBINE EFFICIENCY (ZERO TIP LEAKAGE)



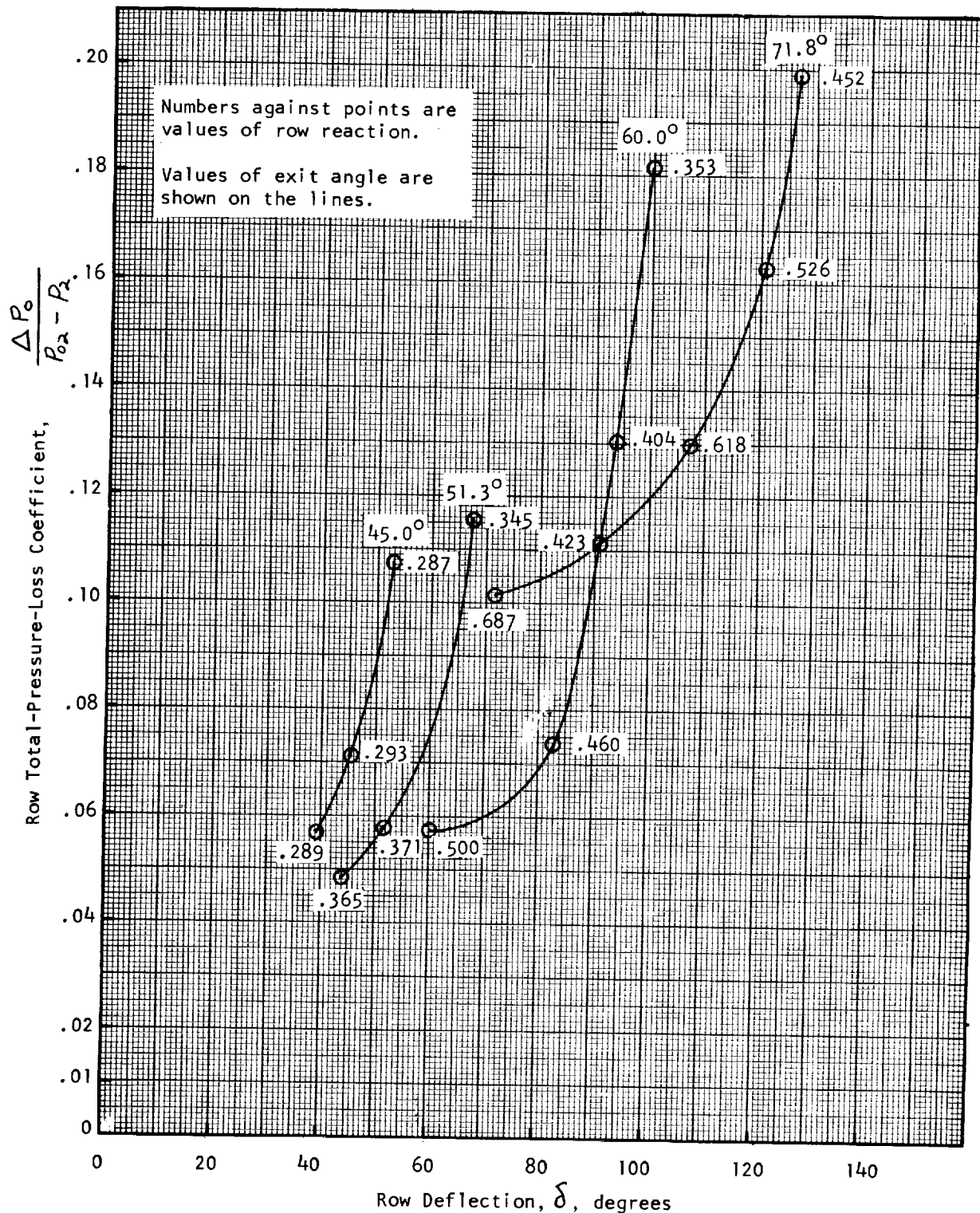


FIGURE 5 - LOSS COEFFICIENTS VERSUS ROW DEFLECTION

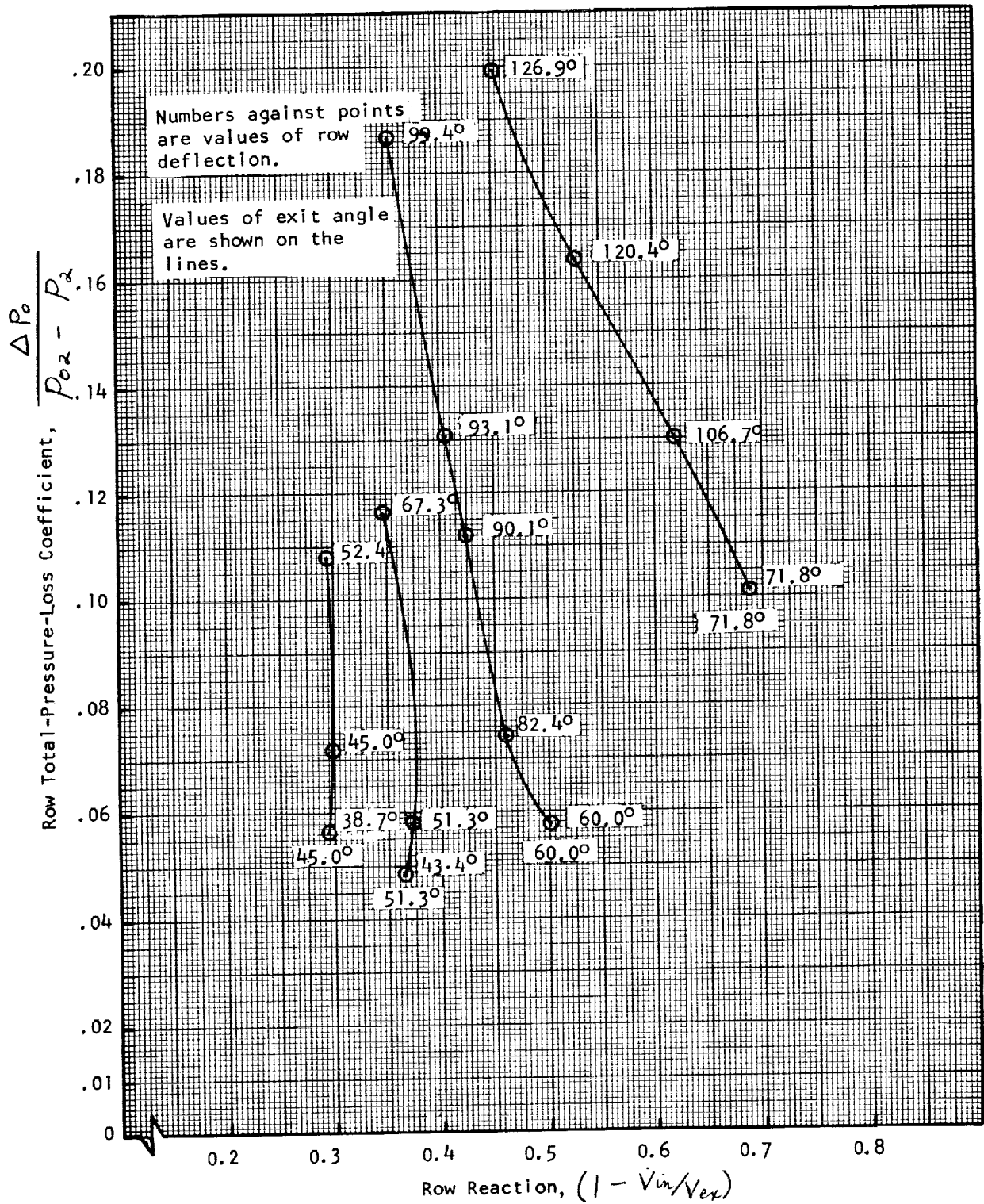


FIGURE 6 - LOSS COEFFICIENTS VERSUS ROW REACTION

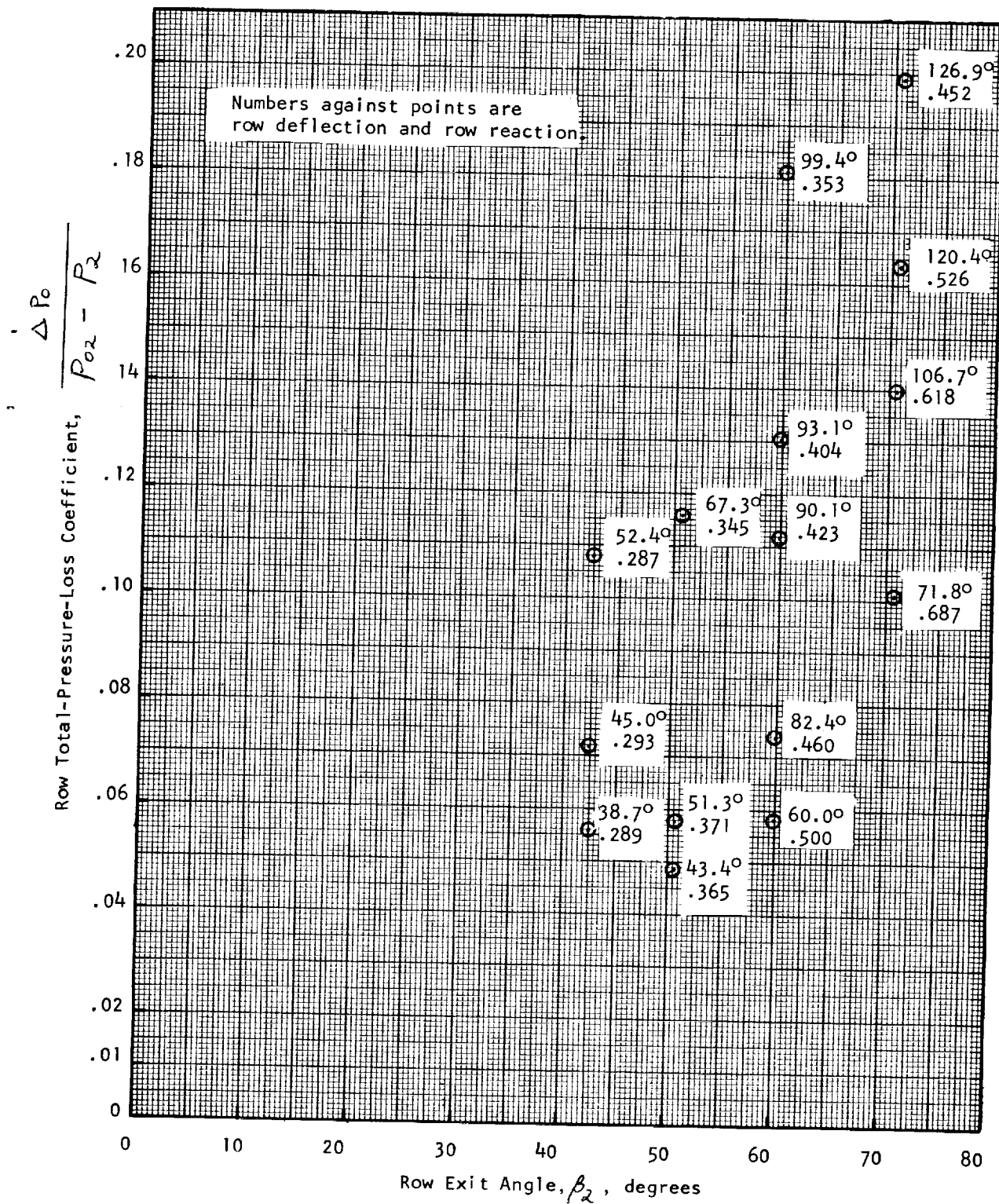


FIGURE 7 - LOSS COEFFICIENTS VERSUS ROW EXIT ANGLE

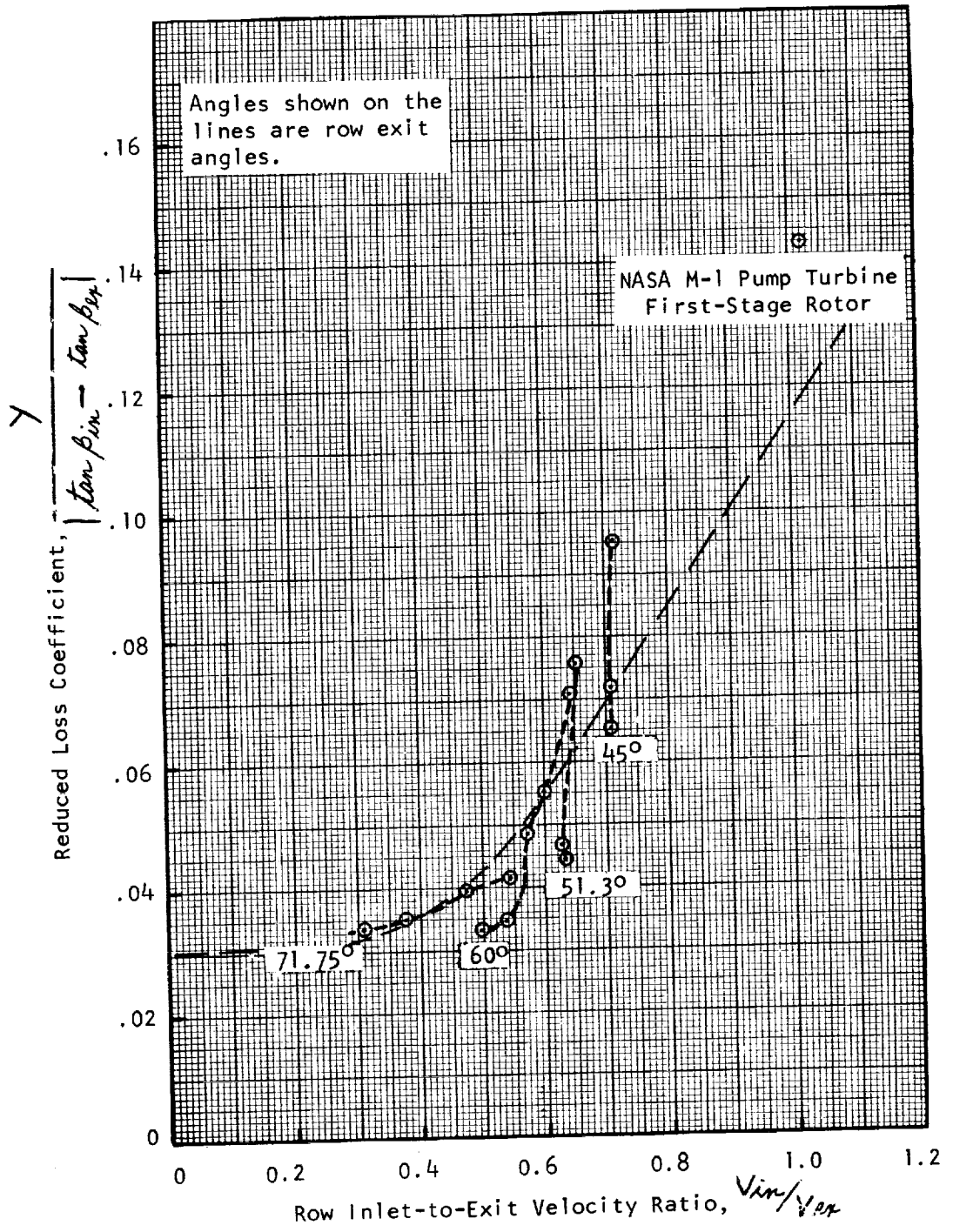


FIGURE 8 - REDUCED LOSS COEFFICIENTS VERSUS VELOCITY RATIO

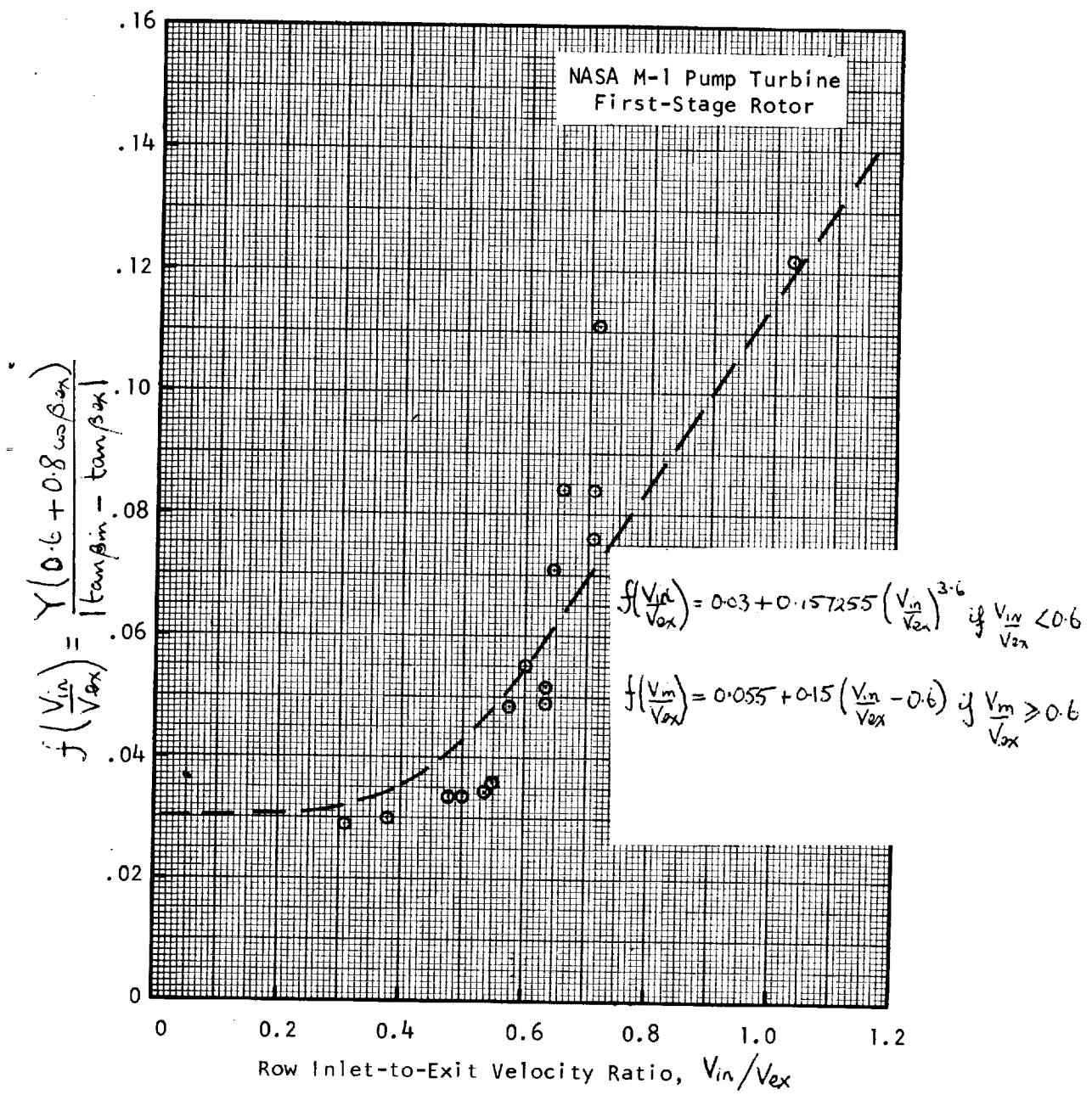


FIGURE 9 - REDUCED LOSS COEFFICIENTS WITH  
ADDITIONAL EXIT ANGLE CORRECTION VERSUS VELOCITY RATIO

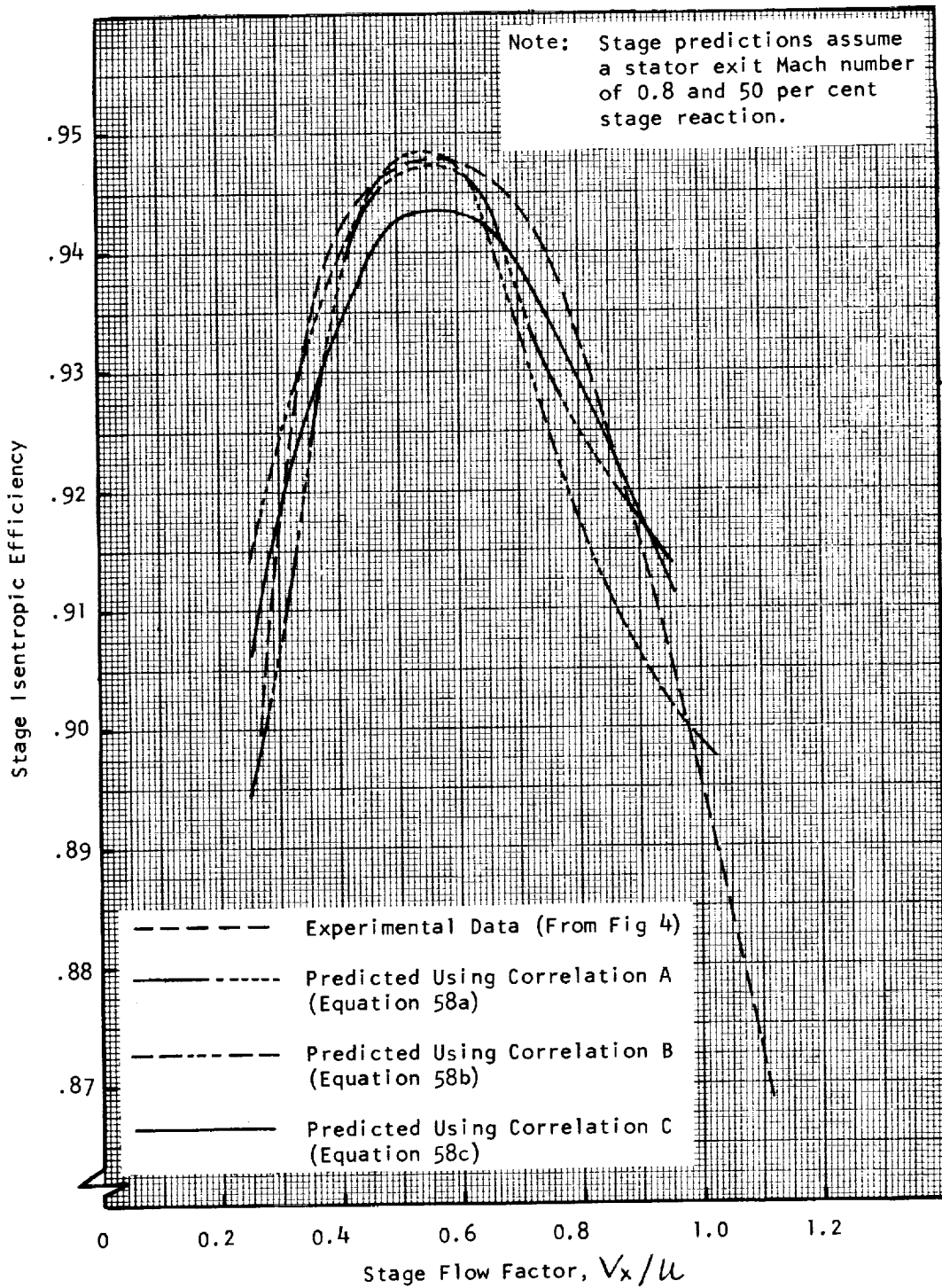


FIGURE 10 - A COMPARISON OF TEST DATA EFFICIENCIES WITH PREDICTION VALUES USING ALTERNATIVE LOSS COEFFICIENT CORRELATIONS ( $g_0 \int c_p \Delta T_c / u^2 = 1.0$ )

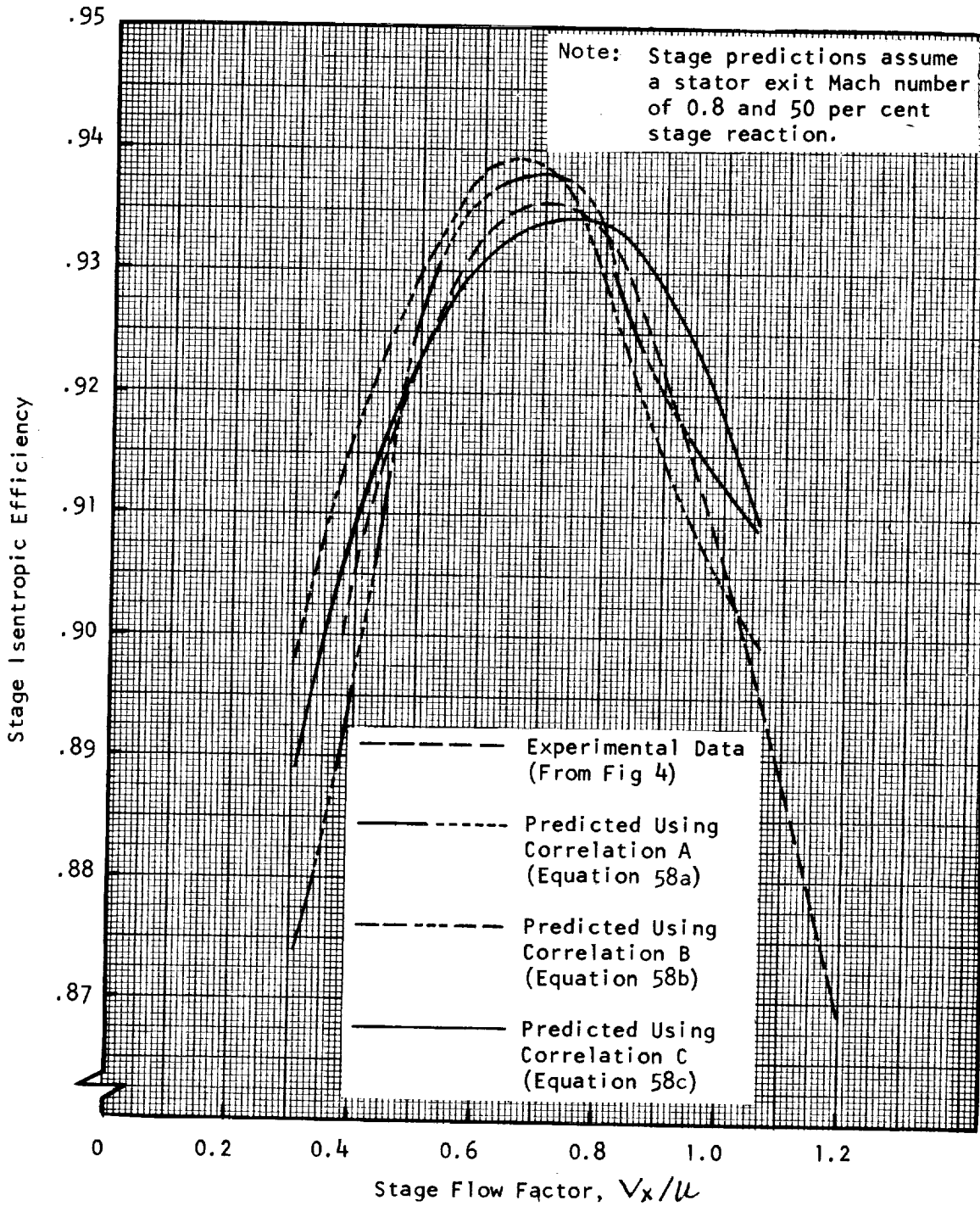


FIGURE 11 - A COMPARISON OF TEST DATA EFFICIENCIES WITH PREDICTION VALUES USING ALTERNATIVE LOSS COEFFICIENT CORRELATIONS ( $g \cdot J \cdot c_p \cdot \Delta T_0 / u^2 = 1.5$ )

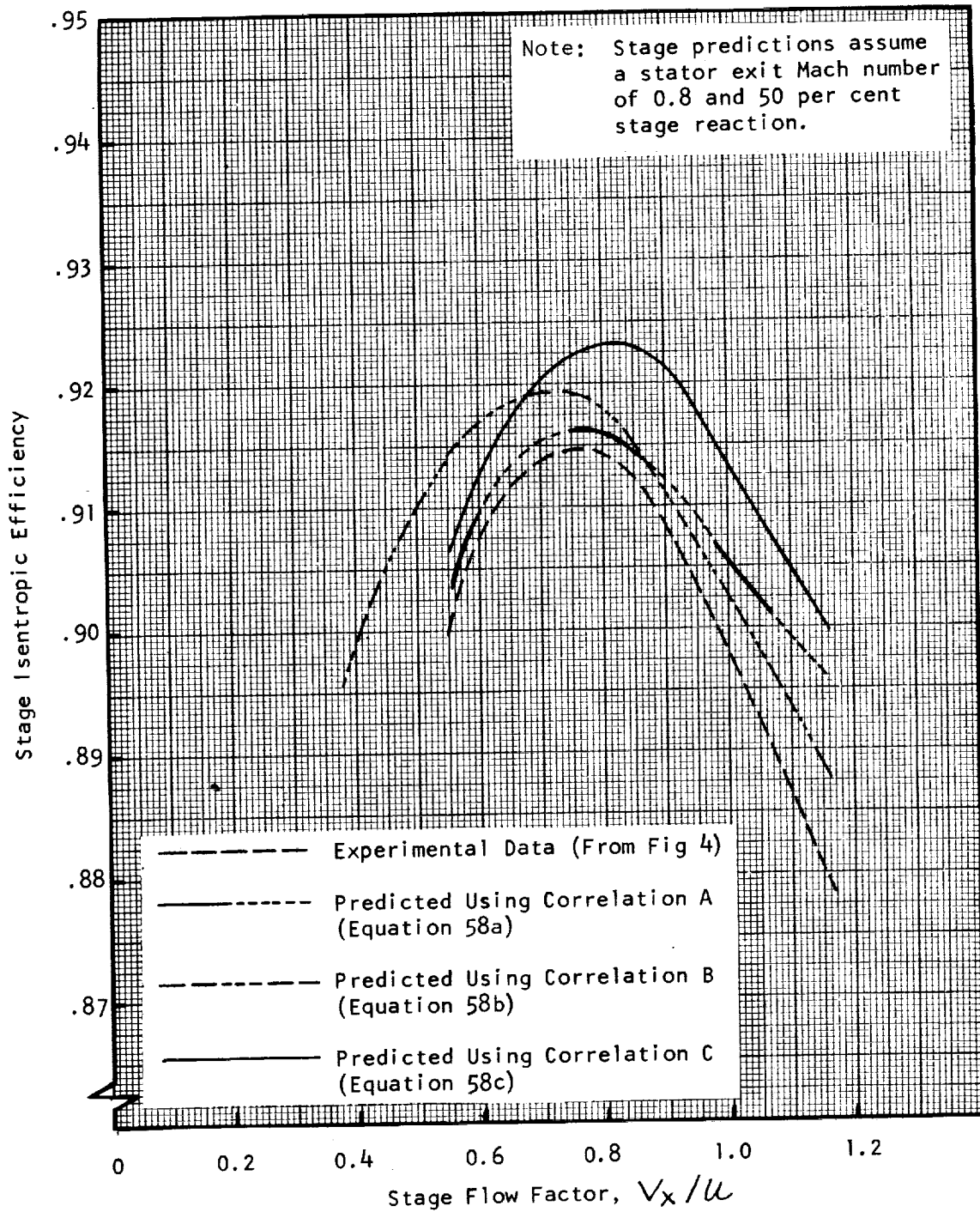


FIGURE 12 - A COMPARISON OF TEST DATA EFFICIENCIES WITH PREDICTION VALUES USING ALTERNATIVE LOSS COEFFICIENT CORRELATIONS ( $g_c \int c_p \Delta T_c / u^2 = 2.0$ )



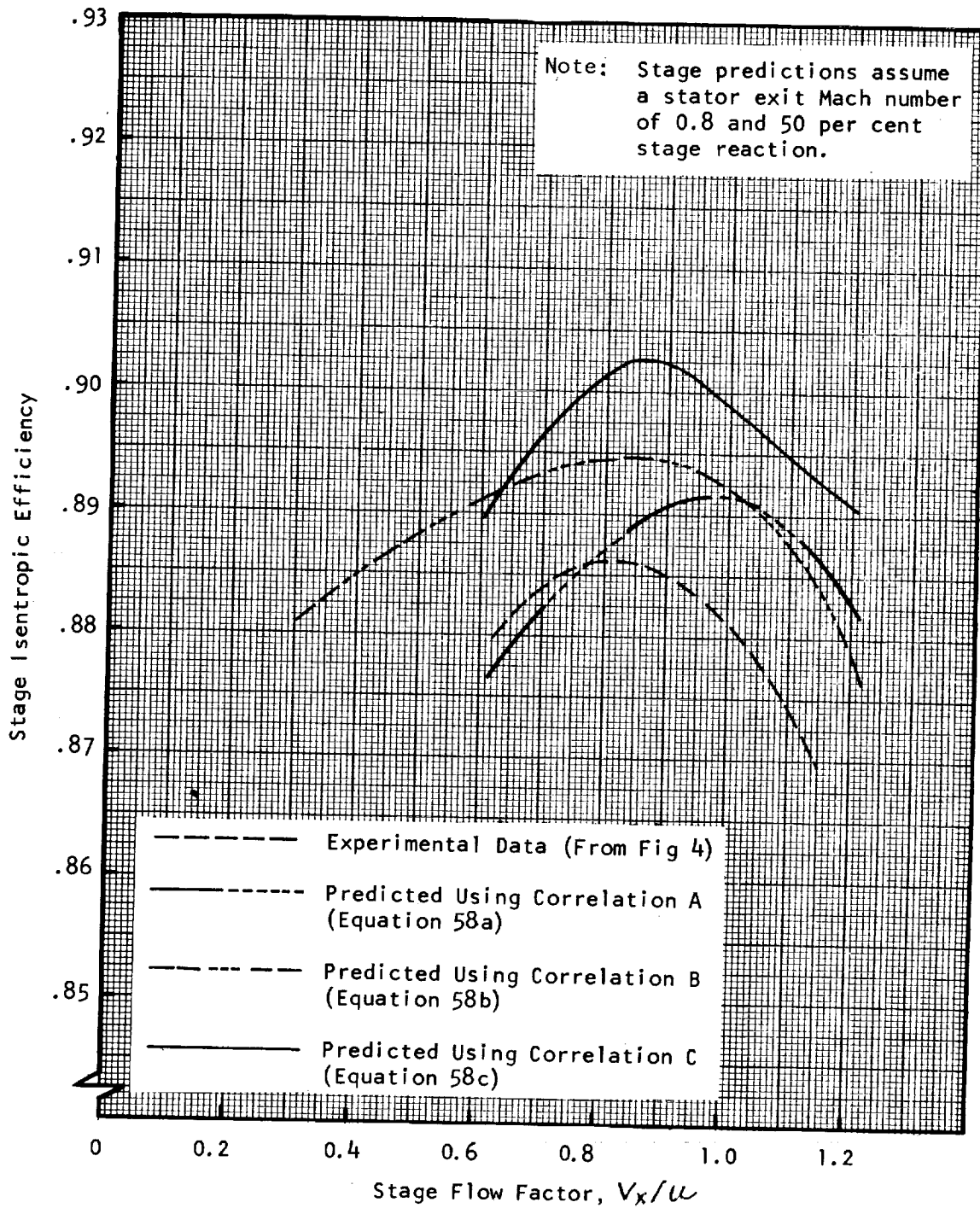


FIGURE 13 - A COMPARISON OF TEST DATA EFFICIENCIES WITH PREDICTION VALUES USING ALTERNATIVE LOSS COEFFICIENT CORRELATIONS ( $g_0 J C_p \Delta T_0 / u^2 = 2.5$ )

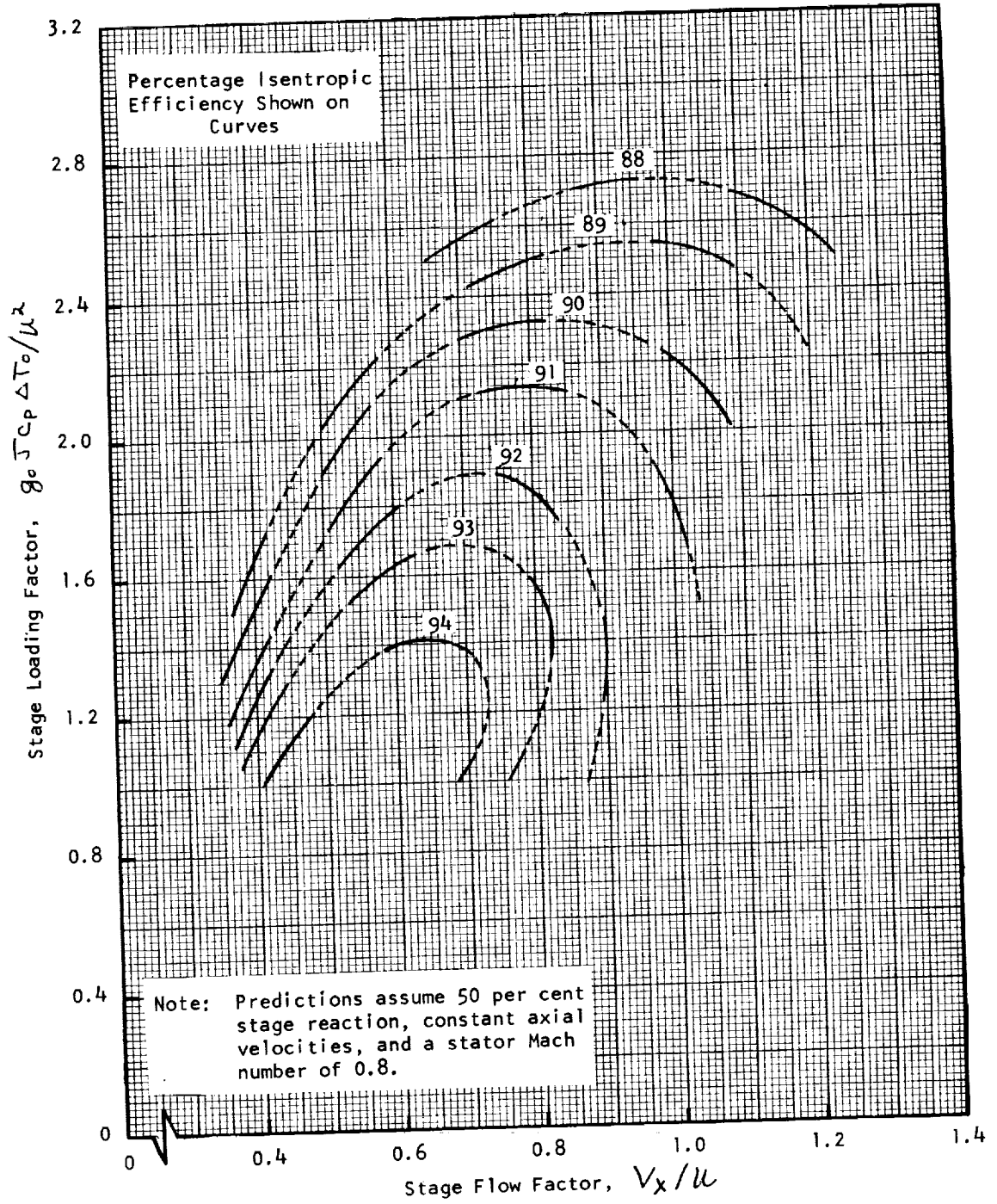


FIGURE 14 - PREDICTED EFFICIENCY CONTOURS  
 BASED ON ROW LOSS COEFFICIENT CORRELATION A

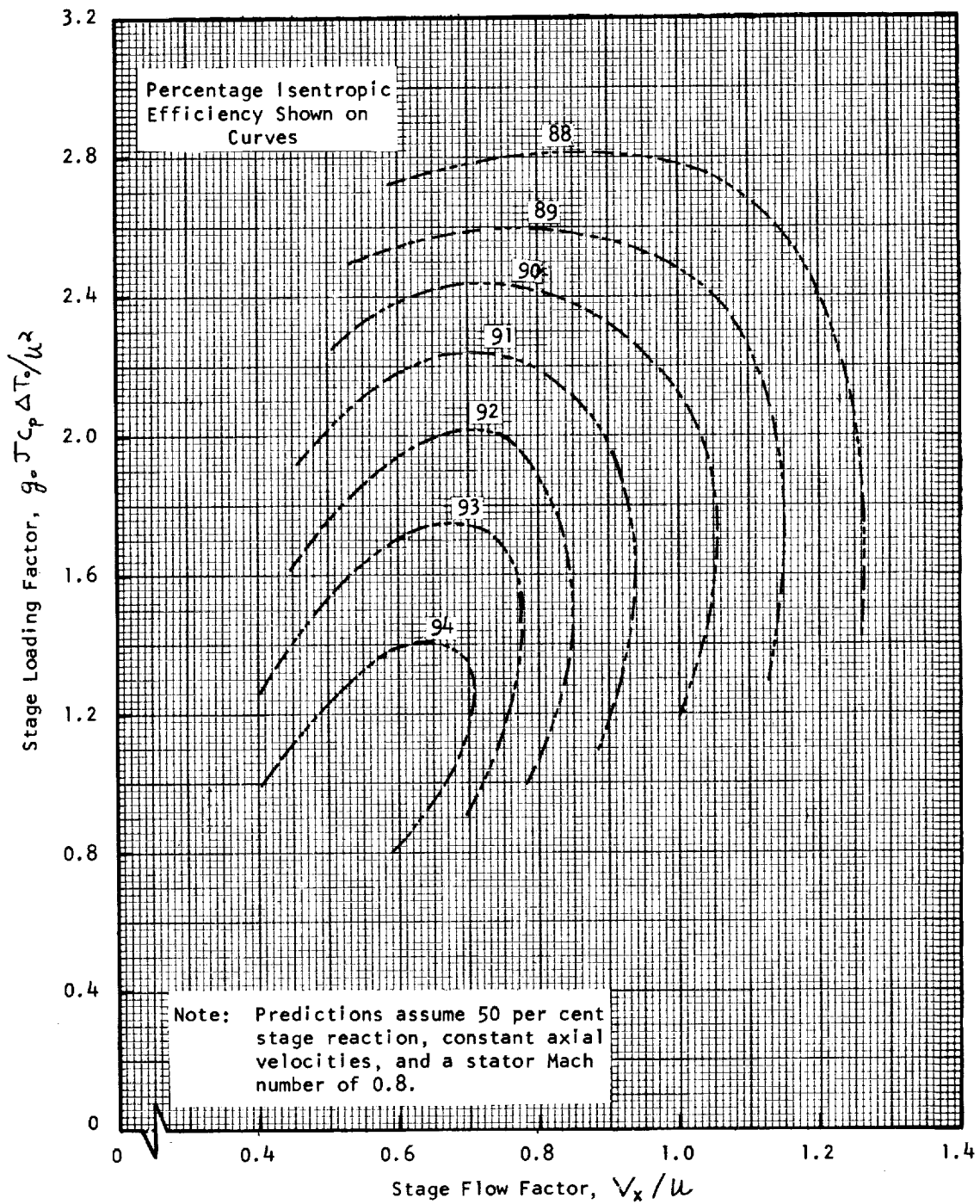


FIGURE 15 - PREDICTED EFFICIENCY CONTOURS  
 BASED ON ROW LOSS COEFFICIENT CORRELATION B

